Impacts of climate and reclamation on temporal variations in CH_4 emissions from different wetlands in China: From 1950 to 2010

Running title: CH_4 from Chinese natural wetlands

Tingting Li[1], Wen Zhang[1,*], Qing Zhang[1], Yanyu Lu[2], Guocheng Wang[1], Zhenguo Niu[3], Maarit Raivonen[4], Timo Vesala[4,5]

[1] LAPC, Institute of Atmospheric Physics, Chinese Academy of Sciences, Beijing, 100029, China

[2] Anhui Climate Center, Hefei, 230031, China

[3] State Key Laboratory of Remote Sensing Science, Jointly Sponsored by Institute of Remote Sensing Applications, Chinese Academy of Sciences and Beijing Normal University, Beijing 100101, China;

[4] Department of Physics, P.O. Box 48, FI-00014 University of Helsinki, Finland

[5] Department of Forest Sciences, P.O. Box 27, FI-00014 University of Helsinki, Finland

Correspondence to: Wen Zhang (Email: zhw@mail.iap.ac.cn, Tel: 86-10-62071389)

Keywords: CH_4 emissions, wetland, modeling, temporal variation, China

Abstract

Natural wetlands are among the most important sources of methane; thus, these areas are important for better understanding long-term temporal variations in atmospheric methane concentration. During the last 60 years, wetlands have experienced extensive conversion and global impacts from climate warming, which makes the estimation of methane emission from wetlands highly uncertain. In this paper, we present a modeling framework, integrating $CH4MOD_{wetland}$, TOPMODEL and TEM models, to analyze the temporal and spatial variations in CH_4 emissions from natural wetlands (including inland marshes/swamps, coastal wetlands, lakes and rivers) in China. Our analysis revealed an increase of 25.5%, averaging 0.52 g m^{-2} per decade, in national CH_4 fluxes from 1950 to 2010, which was mainly induced by climate warming. Higher rates of increasing CH_4 fluxes occurred in northeastern, northern and northwestern China, associated with large temperature increases. However, decreases in precipitation due to climate warming offset the increase in CH_4 fluxes in these regions. The CH_4 fluxes from the wetland on the Qinghai Tibetan Plateau exhibited a lower rate of increase, which was approximately 25% of that simulated in northeastern China. Although climate warming has accelerated CH_4

fluxes, the total amount of national CH_4 emissions decreased by approximately 2.35 Tg (1.91—2.81 Tg), i.e., from 4.50 Tg in the early 1950s to 2.15 Tg in the late 2000s, due to a large wetland loss of 17.0 million ha. Of this reduction, 0.26 Tg (0.24—0.28 Tg) was derived from lakes and rivers, 0.16 Tg (0.13—0.20 Tg) from coastal wetlands, and 1.92 Tg (1.54—2.33 Tg) from inland wetlands. Northeastern China had the largest contribution to this reduction, with a loss of 1.68 Tg. The CH_4 emissions were reduced by more than half in most regions in China except for the Qinghai Tibetan Plateau, where only a 23.3% decrease in CH_4 was observed.

1. Introduction

Atmospheric methane (CH_4) is the second-most important trace greenhouse gas (GHG) after carbon dioxide (CO_2). The direct radiative forcing of CH_4 was calculated to be 0.48 W m^{-2} by IPCC (2007); this value was revised to 0.97 W m^{-2} when its indirect global warming effect was incorporated (IPCC, 2013; Forster et al., 2007; Shindell et al., 2009). The radiative forcing of CH_4 is then 50 times greater than CO_2 over a 100-year period (IPCC, 2013). In 2011, the concentration of atmospheric CH_4 reached 1803.2 ppb, which is 150% greater than that prior to 1750 (IPCC, 2013). However, unlike the rigid temporal increase in atmospheric CO_2, atmospheric CH_4 has exhibited remarkable temporal variations in conjunction with a long-term increasing trend, remaining nearly constant from 1999 to 2006 and then continually increasing after 2007 (Nisbet et al., 2014). However, the temporal variation in the inventory-based estimates of methane emissions exhibited a different trend. Human-derived CH_4 emissions substantially increased (10%) from 2000 to 2005 due to rapid economic growth and increasing demand for food and energy, implying inaccuracies in the inventories and simultaneously offsetting the decreases in natural emissions or a comparable increase in sinks (Montzka et al., 2011).

Natural wetland emissions are the largest as well as the most uncertain source in the global CH_4 budget (Denman et al., 2007; Potter et al., 2006; Whalen, 2005), ranging from 115 (Fung et al., 1991) to 237 Tg CH_4 yr^{-1}, (Hein et al., 1997) and representing 20% to 40% of the global source. It has been frequently stated that half of the world's wetlands were lost during the 20th century (Moser et al., 1996; Revenga et al., 2000). Davidson (2014) reviewed 189 reports of the changes in wetland area and found that the reported long-term loss of natural wetlands was approximately 54–

57% but may have been as high as 87% since 1700 AD. Wetland loss may offset the increase in human-derived CH_4 emissions from 2000 to 2005 (Bousquet et al., 2006).

China has the world's fourth largest wetland area (Wang et al., 2012a). China's natural wetlands consist of a wide variety of types and are representative in the world. In China, natural wetlands have also experienced a serious loss during the past 60 years, attributed primarily to reclamation (An et al., 2007; Niu et al., 2012; Huang et al., 2010; Xu and Tian, 2012). The reclamation occurred not only in inland marshes and swamps but also in lakes, rivers and coastal wetlands (An et al., 2007). Based on remote sensing data, Niu et al. (2012) reported that approximately 33% of the wetlands were lost between 1978 and 2008. An et al. (2007) estimated that 23% of freshwater swamps, 16% of lakes, 15% of rivers, and 51% of coastal wetlands were lost between 1950 and 2000 based on census data. Wetland reclamation essentially reduces CH_4 emissions, but it has not been accounted for in the estimations of the national CH_4 emissions. For example, Streets et al. (2001) estimated the trends of CH_4 emissions from most of the sources without natural wetlands in China. Increased knowledge concerning the effects of climate and reclamation on the long-term national and regional CH_4 emissions from natural wetlands is helpful for understanding the CH_4 budget and the trends of the atmospheric CH_4 concentration.

Most studies estimating the national CH_4 emissions from natural wetlands have involved the extrapolation of site-specifically measured methane fluxes (Wang et al., 1993; Khalil et al., 1993; Jin et al., 1999; Ding et al., 2004; 2007; Chen et al., 2013; Wang et al., 2012b). Induced by the substantial heterogeneity in wetland CH_4 fluxes (e.g., Christensen et al., 2003; Ding et al., 2004; Yang et al., 2006) and the disagreement in data of the wetland area (e.g., Zhao & Liu, 1995; Xu et al., 1995; Wang et al., 2012b; Zhao, 1999), large uncertainties exist in the national wetland CH_4 emissions inventory ranging between 1.7–10.5 Tg CH_4 yr^{-1}. In addition, the measured fluxes may also yield biased estimations when temporally extrapolated to the distant past which had experienced significant climate changes. Compared with site-specific extrapolation, process-based models are capable of reducing the bias by quantifying the impacts of environmental changes on wetland methane emissions in the modelling mechanism. A few modelling studies have simulated the national CH_4 emissions from the inland marshes/swamps of China (Xu and Tian, 2012; Tian et al., 2011). However, in addition to inland marshes/swamps, lakes, rivers and coastal wetlands are also non-negligible methane sources to the national CH_4 budget (Bastviken et al., 2004;

Yang et al., 2011; Chen et al., 2013), and they have also suffered significant reclamation during the past 60 years (An et al., 2007).

The limited information on the changes in wetland area and the spatial details is the first major reason for the large estimation uncertainty of the national inventory. Recently, Niu et al. (2012) developed maps with sufficient details of the natural wetlands (including inland marshes/swamps, lakes, rivers and coastal wetlands) in 1978, 1990, 2000 and 2008, respectively, retrieved from the Landsat and CBERS-02B remote sensing data. In addition, a biogeophysical model validated against the CH_4 flux measurements representative of the wetlands around the world, i.e., $CH4MOD_{wetland}$ (Li et al., 2010), facilitates the long-term modelling of the methane emissions from all types of the natural wetlands in China. The objectives of the present study are (1) to model spatial and temporal changes in CH_4 emissions across China's natural wetlands (including inland marshes/swamps, lakes, rivers and coastal wetlands) from 1950 to 2010 and (2) to quantify the impacts of climate change and reclamation on the CH_4 emissions from the natural wetlands in different regions of China.

2. Materials and Methods

As defined by the Ramsar Convention (Ramsar, Iran, 1971) and the Chinese government (An et al., 2007), natural wetlands include a wide variety of habitats such as marshes, peatlands, floodplains, rivers and lakes, and coastal areas. Following the Ramsar Convention, the primary natural wetland types in this study include coastal wetlands, lakes and rivers, and other types that are defined as inland wetlands (e.g., marshes, swamps, peatlands, and floodplains). We used an integrated modelling framework centered on $CH4MOD_{wetland}$ (Li et al., 2010) to simulate the CH_4 emissions from inland and coastal wetlands. Directly extrapolated field measurements were used to calculate the CH_4 emissions from lakes and rivers (Chen et al., 2013).

2.1 Modelling framework

Fig. 1 shows the modelling framework used in this study. Three models were used with a spatial resolution of 0.5° for the period from 1950 to 2010. The center of the modelling framework is $CH4MOD_{wetland}$ (Li et al., 2010). $CH4MOD_{wetland}$ is a biogeophysical model that aims to simulate the CH_4 production, oxidation and emissions from natural wetlands (Li et al., 2010). This model adopts the rationale of the CH4MOD model which is used to simulate the processes concerning the CH_4

emissions from rice paddies (Huang et al., 1998, 2004, 2006; Zhang et al., 2011). While the sources of methanogenic substrates and the primary regulating factors are essentially different between natural wetlands and rice paddies, sufficient modifications were made so that the model can be used for natural wetlands. In $CH4MOD_{wetland}$, methane production rates are calculated by the availability of methanogenic substrates and the parameterized influences of environmental factors, e.g., soil temperature, soil texture and soil redox potential. The methanogenic substrates are derived from the root exudation of wetland plants and the decomposition of above- and below-ground litters and the soil organic matter. The CH_4 emissions to the atmosphere via diffusion, ebullition and plant transportation are all simulated in the model. Oxidation occurs when CH_4 diffuses to the atmosphere or is transported via the plant aerenchyma.

The model inputs include the soil texture (soil sand fraction, soil organic carbon and bulk density), aboveground net primary productivity (*ANPP*), daily soil temperature, water table depth and salinity. With the modelling outputs of the daily CH_4 emissions (g m^{-2} d^{-1}), we multiplied the CH_4 fluxes by the wetland area in each 0.5 °×0.5 ° grid and summed up the CH_4 emissions from all grids to yield the total national CH_4 emissions.

The validation of $CH4MOD_{wetland}$ against the field measurements of CH_4 fluxes from wetlands across China, Canada and the U.S.A. presents details of the model performance (Li et al., 2010; 2012). At present, however, the insufficiency of the model mechanism, e.g., lacking the influence of thawing permafrost on CH_4 production will result in distorted CH_4 simulations during the winter and freeze-thaw period; dynamics of the water table and the growth of wetland plants, limits its upscaling from fields to regions where no measurements of the water tables and plant biomass are available.

To obtain regional datasets of ANPP, soil temperature and water table depth at the national scale, we used the outputs of the Terrestrial Ecosystem Model (TEM) (Melillo et al., 1993; Zhuang et al., 2004; 2006; 2007; 2013) and TOPMODEL (Beven and Kirby, 1979) to integrate into $CH4MOD_{wetland}$.

The TEM model is also a process-based biogeochemistry model that couples carbon, nitrogen, water, and heat processes in terrestrial ecosystems to simulate ecosystem carbon and nitrogen dynamics. This model has been widely used to investigate regional and global NPP (e.g., Melillo et al., 1993; Cramer et al., 1999;

McGuire et al., 1992). With this model framework (Fig. 1), the soil temperature and net primary productivity (NPP) outputs from the TEM model were used to drive $\text{CH4MOD}_{\text{wetland}}$. The fraction of ANPP to NPP was determined based on Gill and Jackson (2003). Further descriptions of the model and the inputs are described in Zhuang et al. (2013).

TOPMODEL is a rainfall-runoff model that is designed to work at the scale of large watersheds using the statistics of topography. In previous research (Bohn et al., 2007; Kleinen et al., 2012; Lu and Zhuang et al., 2012; Zhu et al., 2013), TOPMODEL has been widely used to simulate water table variations in natural wetlands. The TOPMODEL inputs included soil moisture and the topographic wetness index (Fig. 1). More details on simulating water table depth using TOPMODEL are provided in Supplementary Material S1.

Previous studies (Atkinson and Hall, 1976; King and Wiebe, 1978; Bartlett et al., 1985; 1987; Magenheimer et al., 1996) have indicated that methane emissions from various coastal salt marshes in the temperate zone vary with salinity. To improve the capacity to simulate methane emissions from coastal wetlands, we adopted the relationship between salinity and methane fluxes according to Poffenbarger et al. (2011):

$$f(s) = 10^{a \times s} \tag{1}$$

where $f(s)$ represents the effect of salinity on CH_4 production, s is the salinity (psu, practical salinity unit), and a is an empirical constant.

2.2 Model calibration

The natural wetlands in China have complex plant species. Considerable spatial variations in fluxes related to vegetation have been found (Ding et al., 2004; Hirota et al., 2004; Song et al., 2007; Duan et al., 2005; Huang et al., 2005). Such variations have been ascribed to the differences in NPP, the capacity of transferring labile organic carbon into anoxic environments, and the capacity for the plant transport and oxidation of CH_4 (Berrittella and Huissteden, 2011). Sufficient calibration and parametrization of the vegetation parameters in the model is important for reliably reproducing CH_4 emissions at wetland sites. *Carex* and *Phragmites* are dominant plant species in Chinese natural wetlands (Lang & Zu, 1983). Previous site measurements (Table S1) on the wetlands with *Carex* and *Phragmites* provide the data for model calibration and validation.

The recalibrated parameters of $\text{CH4MOD}_{\text{wetland}}$ in the present study are mainly related to vegetation, e.g., the proportion of the roots to the total production (f_{root}), the vegetation index (VI), the fraction of CH_4 oxidized during plant-mediated transport (P_{ox}) and the fraction of available plant-mediated transport (T_{veg}). f_{root} and T_{veg} were obtained from the literature (please see Table S2). VI is a vegetation index that can identify the relative differences in methane production among vegetation types, and P_{ox} recognizes the different fractions of CH_4 oxidized when transported by different plant species. Both VI and P_{ox} were calibrated to account for the differences between plant species.

In our previous studies, we parameterized VI and P_{ox} using the CH_4 flux measurements collected from the Sanjiang Plain (SJ site in Table S1) in Region I (Fig. 2), where the dominant plant species is *Carex* (Supplementary Material S3) (Li et al., 2010, 2012). In this study, VI and P_{ox} were recalibrated for the wetlands dominated by *Phragmites* (Table S2). We parameterized VI and P_{ox} by minimizing the differences between the observed and simulated fluxes at Wuliangsu Lake in Inner Mongolia (WLS site in Table S1). By setting an increment of 0.1 for VI and P_{ox}, the model was run for all combinations of VI within the range 0.5—3.0 and P_{ox} within the range 0.1—1 until the root-mean-square error (RMSE) between the simulated and observed CH_4 fluxes was minimized. After setting VI and P_{ox}, the empirical constant of the salinity influence a [Eqn. (1)] was calibrated by minimizing the root-mean-square error (RMSE) between the observed and simulated fluxes at a coastal wetland on Chongming Island in Shanghai Province (CMI site in Table S1). Table S2 shows the detailed definition and values of the model inputs and parameters for the wetland sites.

2.3 Model validation

After model calibration, model validation is performed to evaluate if the model is suitable to extrapolate up to large scales. We used observations (different from the data used to calibrate the model) to validate the model at the “site-scale” using individual $\text{CH4MOD}_{\text{wetland}}$ simulations and at the “grid-scale” using the proposed model framework (Fig. 1). More details regarding the “site-scale” and the “grid-scale” validations are described in Supplementary Material S2.

The “site-scale” validation were carried out at the wetland sites on the Sanjiang Plain (Figure S1a, S1b), the Ruoergai Plateau, (REG in Table S1; Figure S1d, S1e), the Haibei alpine marsh (HB in Table S1; Figure S1g), the Zhalong wetland (ZL in

Table S1; Figure S1i) and the Liao River delta (LRD in Table S1; Figure S1k). The comparison of the simulated versus the observed monthly CH_4 fluxes resulted in an R^2 of 0.79, with a slope of 0.86 and an intercept of 0.73 (n=41, p<0.001) (Figure S2a). The RMSE, mean deviation (RMD) and the model efficiency (EF) between the simulated and observed monthly CH_4 fluxes were 48.5%, 0.9% and 0.78, respectively.

The "grid-scale" validation showed that the integrated model framework ($CH4MOD_{wetland}$/TEM/TOPMODEL) (Fig. 1) was able to simulate the seasonal variations in monthly CH_4 emissions at the SJ (Figure S1c) and LRD (Figure S1l) sites. Although there are some underestimations in the CH_4 fluxes were predicted by the model framework for the other 3 sites (Figure S1f, S1h and S1j), the measured monthly CH_4 fluxes fell in or near the range of the modeled CH_4 emissions (Figure S2b). For the "grid-scale" validation, the regression of simulated versus observed monthly CH_4 emissions resulted in an R^2 of 0.79, with a slope of 0.84 and an intercept of -0.11 (n=41, p<0.001). The RMSE, RMD and EF between the simulated and observed monthly CH_4 fluxes were 51.3%, -17.8% and 0.75, respectively, for the integrated model framework.

2.4 Upscaling of the model framework

Lang and Zu (1983) divided the Chinese wetlands into five regions according to the environmental conditions and dominant vegetation type (Fig. 2). For national model simulations of CH_4 fluxes, we adopted the regional divisions of Lang and Zu (1983) and assigned the vegetation-related parameters of $CH4MOD_{wetland}$ with the calibrated values in Table S2. For more details about the climate, soil and vegetation type of the regions, please see Supplementary Material S3.

The wetland sites (Table S1) that we used for the calibration and validation are representative in the regions (Fig. 2). For example, the SJ site is a typical freshwater marsh with *Carex* plants, which is widely distributed in northeastern China. The floodplain with *Phragmites* beside rivers and lakes such as the WLS site are the main wetland type in Region III and Region IV. The model parameters at SJ and HB (Table S2) were assigned to Region I and Region II, respectively. The parameters for WLS (Table S2) were assigned to Region III and Region IV. The model parameters for REG (Table S2) were allocated to Region V because this wetland is located at the edge of this region. The value of a in [Eqn. (1)] was assigned to the coastal wetlands.

We established gridded (0.5°×0.5°) and geo-referenced time-series input datasets of climatic factors (including daily temperature, precipitation, humidity, and solar radiation), soil data (including soil sand percentage, soil bulk density, soil organic carbon and soil moisture) and salinity data for all of China. The climate and soil texture data were used to drive the TEM model (Fig. 1). The soil moisture and topographic wetness index data were used as inputs for TOPMODEL (Fig. 1). Then, CH4MOD$_{\mathrm{wetland}}$ ran with the *ANPP*, soil temperature (the outputs of TEM), water table depth (the output of TOPMODEL), soil texture, and salinity data in each grid cell to simulate the CH_4 fluxes (Fig. 1). The total CH_4 emission from each grid cell was calculated as the product of the CH_4 fluxes and the gridded wetland area.

2.5 Uncertainty analysis

Uncertainty in the estimated regional CH_4 emissions from natural wetlands may originate from many reasons. In this study, we focused on the uncertainties induced by the inputs of *ANPP*, the water table depth and the soil sand fraction using the extreme condition approach for uncertainty propagation (Du and Chen, 2000; Li et al., 2012). The Monte Carlo method has been widely used in uncertainty analysis. However, because the Monte Carlo method is computationally expensive, the extreme condition approach was used instead in the regional simulations (Li et al., 1996; 2004; Giltrap et al., 2010; Kesik et al., 2005). Compared with the Monte Carlo method, the extreme condition approach provides no information on the statistical properties of the uncertainty, but it can provide hints of the uncertainty ranges with a much lower modelling cost. Li et al. (2004) reported that the uncertainty ranges produced by the extreme condition approach (MSF method in the study) covered 97%, 98%, and 61% of the uncertainties produced by the Monte Carlo method for the CO_2, CH_4, and N_2O from rice paddies, respectively.

In this study, we designed eight scenarios with a cross combination of the maximum and minimum values of *ANPP*, water table depth and the soil sand fraction, ±10% from their baseline values. This represents the average range of the measured *ANPP* as well as the soil sand fraction at the sites (Table S1). For the baseline estimate, we used the *ANPP* from TEM model, the water table depth from TOPMODEL and the input soil sand fraction to drive the CH4MOD$_{\mathrm{wetland}}$ from 1950 to 2010. Then we randomly selected the maximum and minimum *ANPP*, water table depth and the soil sand fraction in each grid as a scenario. There are eight scenarios (e.g. maximum ANPP, maximum water table depth, minimum soil sand fraction) from the random combination. CH4MOD$_{\mathrm{wetland}}$ ran eight rounds with each of the eight scenarios. The minimum and maximum values of the eight simulated CH_4 fluxes were considered to be the range of the modeling uncertainty.

2.6 Estimate CH_4 emissions from lakes and rivers

In this study, we followed Chen's method (Chen et al., 2013) to calculate the CH_4 emissions from lakes and rivers across China [Eqn. (2)). Lakes can be found in five major regions in China: the plains of eastern China, the Qinghai-Tibetan Plateau, the Yunnan-Guizhou Plateau, the Mongolia-Xinjiang Plateau, and the Northeast China Plain (Wang and Dou, 1998).

$$CH4_{regional} = \sum_i \sum_j \sum_k f_{ijk} \times A_{ijk} \times D_{ijk} \qquad (2)$$

i is the lake region, j is the growing season and non-growing season (between the different regions), and k is the different zones (pelagic zone and/or littoral zone). f_{ijk} is the seasonal mean CH_4 fluxes under the conditions of i, j, and k (listed in Table S3). A_{ijk} is the lakes' area, and D_{ijk} is the duration of the growing and non-growing season or the unfrozen season. $CH4_{regional}$ is the regional CH_4 emissions from lakes.

The average area-weighted CH_4 flux was calculated as:

$$CH4_{flux} = \frac{CH4_{regional}}{\sum_i \sum_j \sum_k A_{ijk}} \qquad (3)$$

Uncertainties in the estimation were due to an inaccuracy in the fraction of the littoral zones of the lakes, which was assumed to be from 5% to 12% for all lakes in China based on a preliminary estimate (Chen et al., 2009).

When [Eqn. (2)] was used to calculate the regional CH_4 emissions from rivers, f_{ijk} was assumed to equal the value in the pelagic zone because no data were available.

2.7 Time series of the wetland area

In this study, we tried to obtain the gridded time series of historical wetland area datasets. However, gridded wetland maps were only available for 1978, 1990, 2000 and 2008 (Niu et al., 2012). The initial wetland area of 1950 was estimated with the historical census data as well as remotely sensed wetland maps. In the historical census data, the wetland area had been decreasing during the past 60 years, especially before the early 1990s, until the Chinese government began restoring the degraded wetlands (An et al., 2007).

Northeastern China (Region I in Fig. 1) has received more attention because it is abundant in wetlands but has undergone dramatic wetland loss since 1950. We separated the Sanjiang Plain from China and used more detailed and accurate data (Liu and Ma, 2000; Li et al., 2012; Huang et al., 2010; Ding et al., 2004) to build the decadal time series of the change in wetland area in the region.

The method for obtaining the gridded wetland map for 1950 was based on both Niu et al. (2012) and An et al. (2007). An et al. (2007) reported losses of 23.0% of inland wetland areas, 16.1% of lake areas, 15.3% of river areas, and 51.2% of coastal wetland areas between 1950 and 2000 in China. For inland wetlands, we assumed an average annual loss rate between 1950 and 2000 occurring in each inland wetland grid cell. We calculated this annual loss rate based on An's results from between 1950 and 2000. Then, the inland wetland area in each grid cell at 1950 was reverse-extrapolated based on the wetland map for 1978 by Niu et al. (2012) and the above annual loss rate. This method was also used to calculate the changes in lake, river and coastal wetland areas.

2.8 Data sources

We selected seven typical natural wetlands where extensive field measurements were available for the model calibration and model validation of $\mathrm{CH4MOD_{wetland}}$. These sites included two marshes, two floodplains, one peatland and two coastal wetlands (Table S1). The CH_4 emissions were measured weekly or monthly at these sites. Most of the sites have synchronous measurements of the climate and water table depth. Fig. 2 shows the locations of the sites. More detailed site descriptions are provided in Table S1.

The gridded wetland maps of 1950, 1978, 1990, 2000 and 2008 were used in this study. The initial gridded wetland map of 1950 was estimated based on the remote sensing data of 1978 (Niu et al., 2012) and the census data (An et al., 2007) (see section 2.7). The gridded wetland maps for 1978, 1990, 2000 and 2008 were obtained from Niu et al. (2012). The gridded wetland maps include inland marshes/swamps, coastal wetlands, lakes and rivers. The floodplains and rivers as river wetlands were combined in Niu et al. (2012); however, because floodplains are always dominated by vascular plants, we combined floodplains with inland marshes/swamps as the inland wetland category. The fraction of floodplains was based on original satellite data (Z. G. Niu, personal communication, 2013).

The climate datasets from 1950 to 2010 used for driving the TEM model were developed from the latest monthly air temperature, precipitation, vapor pressure, and cloudiness datasets from the Climatic Research Unit (CRU TS 3.10) of the University of East Anglia in the United Kingdom (Harris et al., 2014).

The monthly soil moisture data from 1950 to 2010 were from Fan and van den Dool (2004) (http://www.cpc.ncep.noaa.gov/soilmst/leaky_glb.htm). We used the linear interpolation to develop the daily soil moisture data from 1950 to 2010.

The soil texture data were derived from the soil map of the Food and Agriculture Organization (FAO, 2012). Soil sand fraction data were used as inputs to CH4MOD$_{\mathrm{wetland}}$, whereas soil texture data were used to assign the texture-specific parameters to each grid cell in the TEM model (Zhuang et al., 2013). The soil organic carbon content and the reference bulk density in wetland soils were from the Harmonized World Soil Database (HWSD) (FAO, 2008).

The plant phenology and *ANPP* from 1950 to 2010 were from the TEM outputs data. The vegetation map of IGBP was referenced to specify the vegetation parameters for CH4MOD$_{\mathrm{wetland}}$ and TEM. The map was derived from the IGBP Data and Information System (DIS) DISCover Database (Belward et al., 1999; Loveland et al., 2000). The 1 km × 1 km DISCover dataset was reclassified into the TEM vegetation classification scheme and then aggregated to a resolution of 0.5°×0.5°.

The topographic wetness index data were from the HYDRO1k Elevation Derivative Database, which was developed by the U.S. Geological Survey Earth Resources Observation and Science (EROS) Center (http://gcmd.nasa.gov/records/GCMD_HYDRO1k.html) (USGS, 2000). The global monthly salinity from 1950 to 2010 was from the World Ocean Atlas 2009 (Antonov et al., 2010).

3. Results

3.1 Changes in CH_4 fluxes from 1950 to 2010

The temporal change in CH_4 fluxes (CH_4 emissions per wetland area) were primarily driven by climate changes. In this section, we analyze the seasonal and inter-annual variations in CH_4 fluxes from the inland wetlands and the coastal wetlands from 1950 to 2010.

Fig. 3 shows the seasonal variations of the modeled average CH_4 fluxes from 1950s to 2010s. A consistent pattern of the CH_4 flux peak occurred at the end of July across all regions and decades (Fig. 3). The CH_4 flux peaked coincidently with the highest NPP and temperature of the seasons. CH_4 fluxes were very low in January and February, especially in northern China and in the Qinghai Tibetan Plateau (Fig. 3a, b and c), when the soil froze. In the warmer regions, such as Region V, CH_4 fluxes were much greater (Fig. 3e). The intra-annual changes of CH_4 fluxes were highest in

Southern China (Region V), ranging from 6.38—7.37 mg m^{-2} h^{-1} (Fig. 3e), followed by the Northeastern China (Region I), ranging from 6.35—7.24 mg m^{-2} h^{-1} (Fig. 3a). The Qinghai Tibetan Plateau (Region II) had the lowest intra-annual change of 1.72—1.98 mg m^{-2} h^{-1} (Fig. 3b). There were also the obviously enhanced intra-annual variations of the CH_4 fluxes in all regions in response to the climate warming from 1950s to 2000s (Fig. 3). The intra-annual variations were the highest in 2000s in all of the regions. But the lowest variations occurred in 1970s in region I, II, III (Fig. 3a, b and c) and in 1960s in regions IV, V.

Fig. 4f provides the inter-annual variations and trends in the national annual CH_4 fluxes in China. The national annual CH_4 fluxes significantly increased over the last 60 years, especially since 1980s. The national annual CH_4 flux was 16.9 g m^{-2} yr^{-1} in 1950 and increased to 21.2 g m^{-2} yr^{-1} in 2010, with the average rate of 0.52 g m^{-2} per decade and a total increase of 26% during the period from 1950 to 2010. The annual CH_4 fluxes fluctuated between 16.0 g m^{-2} yr^{-1} and 19.0 g m^{-2} yr^{-1} before 1980, then increasing rapidly in the 1990s. The highest annual CH_4 flux (22.5 g m^{-2} yr^{-1}) occurred in 1998, whereas the lowest (15.7 g m^{-2} yr^{-1}) occurred in 1954.

The estimated annual CH_4 fluxes in different regions are illustrated in Fig. 4a, b, c, d and e. The regions with the largest CH_4 fluxes are Northeastern China (Region I, with an average annual mean of 24.8 g m^{-2} yr^{-1}; Fig. 4a) and Southern China (Region V, with an average annual mean of 20.1 g m^{-2} yr^{-1}; Fig. 4e). On the Qinghai Tibetan Plateau (Region II), the simulated CH_4 fluxes exhibited the lowest fluxes (Fig. 4b), with an average annual mean of 6.2 g m^{-2} over the same period, which was lower than Region I by approximately 75% (Fig. 4a). Compared with Region I, the average CH_4 fluxes in Inner Mongolia and northwestern China (Region III) and over the North China Plain and the Middle-Lower Yangtze Plain (Region IV) were lower by 46% to 64% during the past 60 years.

Fig. 4 also provides the trends in the annual CH_4 fluxes in different regions. Except for Region IV (Fig. 4d; $p>0.05$), the annual CH_4 fluxes exhibited significant increases in other regions (Fig. 4a,b,c,d and e; $p<0.001$). The greatest rate of increase in CH_4 fluxes occurred in Region I, i.e., 0.67 g m^{-2} per decade (Fig. 4a), followed by Region V and Region III, i.e., 0.54 g m^{-2} per decade (Fig. 4e) and 0.42 g m^{-2} per decade (Fig. 4c), respectively. In Region IV, the rate of increase in CH_4 fluxes was 0.50 g m^{-2} per decade, although this rate was not significant (Fig. 4d). The smallest rate of increase occurred in Region II (Fig. 4b), i.e., approximately 25% of the rate for Region I (Fig. 4a).

The modeled five-year CH_4 fluxes exhibited linear trends that closely follow the trends in air temperature in Region I (Fig. 5a), Region II (Fig. 5b), Region III (Fig. 5c) and Region V (Fig. 5e), suggesting that during the past 60 years, the increased CH_4 fluxes were primarily driven by the climate warming. The contribution of precipitation to the trends in CH_4 fluxes differed among the regions. During the past 60 years, Region I and Region III experienced temperature increases by 0.29 ℃ per decade and 0.34 ℃ per decade, respectively. The warming trend resulted in CH_4 fluxes increasing by 0.67 g m^{-2} per decade (Fig. 4a) and 0.42 g m^{-2} per decade, respectively (Fig. 4c). In Region I, the CH_4 fluxes were predominantly positively correlated with air temperature (R^2=0.35, p<0.001) (Fig. 5a). Although no correlation was found between the CH_4 fluxes and the precipitation in Region I, the linear precipitation decrease of 38.3 mm per decade (p<0.001) may have offset the increase in CH_4 fluxes due to the air temperature (Fig. 5a) before 1980. The linear precipitation decrease of 1.7 mm per decade (p=0.4, not significant) in Region III may also have a negative impact on CH_4 fluxes (Fig. 5c). CH_4 fluxes in Region II showed a positive correlation with both temperature and precipitation (Fig. 5b). A slight temperature increase of 0.19 ℃ per decade and precipitation increase of 6.7 mm per decade resulted in a flux increase of 0.17 g m^{-2} per decade. In Region V, the positive correlation between CH_4 fluxes and temperature was more significant than with precipitation (Fig. 5e), suggesting that the temperature was the dominant factor in the acceleration of CH_4 fluxes during the past 60 years. The increase in the precipitation, at a rate of 16.6 mm per decade, though not significant (p=0.24), may have benefited the CH_4 fluxes in this region. In Region IV, CH_4 fluxes were less responsive to temperature than precipitation (Fig. 5d). The increase in temperature also promoted CH_4 fluxes to increase at a rate of 0.50 g m^{-2} per decade (Fig. 4d).

Inter-annual or inter-decadal variations in CH_4 fluxes were found to be closely aligned with variations in precipitation (Fig. 5). The lowest CH_4 fluxes usually accompanied with the periods of low precipitation. For example, the lowest CH_4 fluxes and precipitation occurred simultaneously during the period 1980—1985 in Region IV (Fig. 5d) and the period 1965—1970 in Region V (Fig. 5e). In Region I, the five-year averaged CH_4 fluxes showed a trend that was synchronous with the five-year average precipitation trend (Fig. 5a), decreasing before 1980 and then increasing until 1995. In Region I and Region II, there was excessive amounts of precipitation in the 1990s (Fig. 5a) and 2000s (Fig. 5b) in conjunction with the relatively high air temperatures, which resulted in the highest CH_4 fluxes. In contrast, when the greatest amount of precipitation occurred (Fig. 5c: from 1955 to 1960 in Region III, Fig. 5d: from 1960 to 1975 in Region IV, and Fig. 5e: from 1970 to 1975 in Region V), the CH_4 fluxes remained low due to the lower air temperatures.

3.2 Changes in natural wetlands area

The total wetland area in China was approximately 35.6 million ha in 1950 (Table 1). There had been 17.0 million ha wetland loss from 1950 to 2010, mostly during the first 50 years when the wetland areas decreased by 16.1 million ha. Since 2000, wetland loss has been limited (Table 1).

A tremendous wetland loss of 7.8 million ha occurred in Region I, accounting for approximately 45.7% of the total wetland loss of the nation (Table 1). Compared with 1950, the wetland areas decreased by 56.9%, 24.6%, 48.4%, 65.3% and 46.7% in Region I, Region II, Region III, Region IV and Region V (Table 1), respectively.

Among the wetland types, the inland wetlands underwent the major part of the area loss with 10.3 million ha from 1950 to 2010, accounting for 60.6% of the total wetland loss. More than 95% of the inland wetland loss occurred in Region I, Region II and Region III (Table 1). In contrast, coastal wetland loss occurred primarily in Eastern and Southern China (Region IV and Region V in Table 1). The coastal wetland losses were 68.5% in 2008 compared to the area in 1950. The total area loss was 4.94 million ha for lake and river wetlands between 1950 and 2008. Substantial loss of lakes/rivers occurred in Eastern China (Region IV).

3.3 Changes in the regional CH_4 emissions due to climate change and wetland loss

Along with the wetland loss, the CH_4 emissions decreased by approximately 2.35 Tg (1.91—2.81 Tg) in China’s wetlands, i.e., from 4.50 Tg in the early 1950s to 2.15 Tg in the late 2000s (Table 1). More than 99% of the CH_4 reduction occurred before 2000 (Table 1).

On a national scale, the wetlands in Region I were the greatest contributor to the decreased CH_4 emissions, corresponding to the significant wetland losses (Table 1) and the oppositely increased CH_4 fluxes (Fig. 2b). In Region I, the CH_4 emissions decreased by 58.3% in the late 2000s compared with the early 1950s, with a loss of 1.68 Tg (1.36—2.03 Tg, Table 1). In other regions, the reduction in CH_4 emissions was 0.13—0.19 Tg, with a loss fraction of 23.3—57.6% (Table 1). Among the regions, the lowest CH_4 reduction occurred in Region II, where only a slight loss in wetlands occurred. The loss of CH_4 emissions was 23.3%, which is comparable to the wetland loss (Table 1).

Among the wetland types, the methane emissions decreased by 54.4%, 62.9% and 37.1% from inland wetlands, coastal wetlands and lakes/rivers, respectively (Table 1). Region I was the most important contributor to the decreased CH_4 emissions, which contributed 85.4% to the regional CH_4 reduction for inland wetlands (Table 1). For the coastal wetlands, substantial CH_4 reduction occurred in Region V. The CH_4 fluxes decreased by nearly 82.4% from the early 1950s to the late 2000s in the coastal wetlands of this region (Table 1). Although the coastal wetland loss was higher in Region IV than in Region V, the CH_4 reduction in Region IV was only 21% of that in Region V (Table 1). This difference was because the CH_4 fluxes in the coastal wetland were 2.4 times greater in Region V than in Region IV (compare Fig. 4e with Fig. 4d).

4. Discussion

4.1 Regional estimates of CH_4 emissions in Chinese wetland

China has the world's fourth largest wetland area (Wang et al., 2012a) and contributes 1.7–10.5 Tg CH_4 yr^{-1} (Khalil et al., 1993; Jin et al., 1999; Ding et al., 2004; Ding and Cai, 2007; Chen et al., 2013; Wang et al., 1993; 2012b). On a national scale, this amount is comparable to coal-bed emissions (5.45 Tg CH_4 yr^{-1}), residential biofuel combustion (2.28 Tg CH_4 yr^{-1}), landfills (4.35 Tg CH_4 yr^{-1}), or biomass burning (1.6 Tg CH_4 yr^{-1}) (Streets et al., 2001) and only slightly less than the emissions from rice cultivation (~8 Tg CH_4 yr^{-1}) (Yan et al., 2009; Li et al., 2006a; Chen et al., 2013; Zhang et al., 2011) or livestock (8.55 Tg yr^{-1} Tg CH_4 yr^{-1}) (Streets et al., 2001).

The simulated CH_4 emissions by $CH4MOD_{wetland}$ demonstrated a 2.35 Tg (1.91—2.81 Tg) reduction on the national scale between 1950 and 2010. Although the CH_4 emissions from natural wetlands accounted for ~30% of that from rice paddies during the 2000s (Yan et al., 2009; Li et al., 2006a; Chen et al., 2013; Zhang et al., 2011), the decrease in CH_4 emission was double the increase in the CH_4 emissions from rice paddies (1.2 Tg in Zhang et al., 2011) over the same period.

Previous studies have estimated the CH_4 emissions from the natural wetlands in China. Depending on the different values of the wetland areas in those studies, ranging from 18.7 to 38 M ha, the CH_4 emission differed between 1.7 Tg and 10.5 Tg between 1990 and 2000 (Table 2) (Wang et al., 1993; 2012b; Khalil et al., 1993; Jin et al., 1999; Chen et al., 2013; Cai, 2012; Zhang et al., 2013). In the present study, we estimated that the CH_4 emissions from wetlands of China were 2.17—3.03 Tg during the same period with an area of 19.5 to 23 M ha.

Previous studies have estimated the national wetland CH_4 emissions by simply extrapolating the field measurements of CH_4 fluxes to the national scale (Wang et al., 1993; 2012b; Khalil et al., 1993; Jin et al., 1999; Ding et al., 2004; Chen et al., 2013; Cai, 2012). The estimations of both Ding et al. (2004) and Chen et al. (2013) were primarily based on measurements from Ruoergai at the eastern edge of the Tibetan Plateau. Chen et al. (2013) used an observation of CH_4 fluxes that was much higher than the observation of Ding et al. (2004) during the 2000s, resulting in substantially higher emissions estimates from the wetlands of the Tibetan Plateau (Table 2). Moreover, the spatial characteristics show that Ruoergai has a higher CH_4 flux (Fig. 3) than other places on the Qinghai-Tibetan Plateau, e.g., Huashixia (5.3—6.7 g m^{-2} yr^{-1}) with an altitude of 4000 m in the central Qinghai-Tibetan Plateau (Jin et al., 1999) and Namuco (0.6 g m^{-2} yr^{-1}) with an altitude between 4718 and 7111 m in the hinterlands of the Qinghai-Tibetan Plateau (Wei et al., 2015). This is because Ruoergai has a lower altitude and continuous flooding (Chen et al., 2008; Hirota et al., 2004). Extrapolating the measurements at the eastern edge of the Tibetan Plateau to the whole plateau would inevitably result in estimation biases. The simulated average CH_4 flux from the Qinghai-Tibetan Plateau in 1990 by $CH4MOD_{wetland}$ is 6.2 g m^{-1} yr^{-1} (5.0—7.2 g m^{-2} yr^{-1}), which is close to the observation at Huashixia and between the observations from Namucuo and Ruoergai.

Extrapolating measurements to the region can only be used to estimate the CH_4 emissions after the 1990s because measurement data were not available for earlier periods. Using the DLEM model, Xu and Tian (2012) (Table 2) inferred a reduction of approximately 1.3 Tg CH_4 from Chinese marshlands between 1949 and 2008 due to marshland conversion and climate change. However, the study of Xu and Tian

(2012) focused only on marshlands (natural wetlands excluding coastal wetlands, lakes and rivers), which is equivalent to the inland wetlands in this study. However, our analysis showed that the coastal wetlands, lakes and rivers represented approximately 40% of the total wetland loss (Table 1) and thus is not negligible. The inclusion of the coastal wetlands, lakes and rivers consolidates the estimation of the long-term changes in the CH_4 emissions from wetlands on regional/national scales.

Moreover, in Northeastern China, the dominant vegetation is *Carex*. However, in Inner Mongolia, northwestern China, the North China plain and the Middle-Lower Yangtze Plain, *Phragmites* represents the primary vegetation type (see Supplementary Material S3). Although *Phragmites* usually has a larger biomass than *Carex*, the CH_4 fluxes are lower (according to a comparison between CH_4 fluxes in the perennial inland wetlands in WLS, ZL and SJ in Fig. S1; Table S1). If the observations of methane fluxes from the marshland dominated by *Carex* are used for the model calibration and used in the regions dominated by *Phragmites* (Xu and Tian, 2012), the national estimation might be overestimated. This is why the CH_4 reduction contributed 21.2% in Northwestern and Northern China (including Region III and Region IV in this study) in the study of Xu and Tian (2012) while the contribution was only 7.3% in this study.

4.2 Temporal variations of CH_4 emissions

The intra-annual and inter-annual CH_4 flux trends are largely influenced by the soil temperature, NPP and water table depth. The simulated seasonal variations of the CH_4 fluxes from the sites agreed with the observed values well (Fig. S1). The lowest CH_4 fluxes occurred during the winter or dry period, and the highest fluxes appeared during the summer and flooding period (Fig. S1). The intra-annual variations in this study (Fig. 3) are similar to the simulated seasonal cycles in West Siberia (Bohn et al., 2015) or the northern Hemisphere (Melton et al., 2013) between 1993—2004, which peak in July or August and are mainly driven by high temperature and NPP. In this study, the simulated mean CH_4 flux during the winter in Northeastern China (0.5 mg m^{-2} h^{-1}, Fig. 3a) is similar to the observations from the *Carex lasiocarpa site* in the Sanjiang Plain between 2002—2004 (Zhang et al., 2005). Yang et al. (2006) reported that the fractions of CH_4 flux in the winter and freeze-thaw period were 2.2%—5.5% and 20.6—30.8% in 2003—2005, respectively. The simulated CH_4 fluxes in Region I during the winter and freeze-thaw period in this study accounted for ~8.6% and

~21.1%, respectively (Fig. 3a). The simulated CH_4 fluxes increased by ~8% during the past 60 years (Fig. 4f), similar to that reported by Zhuang et al. (2004), a CH_4 emissions increase of ~7% between the 1950s and 2000s in the Pan-Arctic region.

4.3 Future trends in CH_4 emissions from Chinese wetlands

According to China's National Assessment Report on Climate Change (Ding and Ren, 2007), compared with the period 1961—1990, there will be a pronounced air temperature increase of 3.6—4.9 ℃ in the A2 and B2 scenarios (IPCC, 2000) by the end of this century in China. And the precipitation is also predicted to increase by 9—11% for the two scenarios by 2100 but with obvious differences among regions (Fig. 5).

Warming is expected to promote CH_4 fluxes from wetlands in the future (Zhuang et al., 2006; Christensen and Cox, 1995; Shindell et al., 2004). The air temperature is expected to increase more rapidly in Northeastern China (Region I), Northwestern China (Region III) and the North China Plain (the inland wetlands in Region IV) (Ding and Ren, 2007), which indicates that there will be a larger promotion of CH_4 fluxes from the inland wetlands in these regions. For the Qinghai Tibetan Plateau (Region II), Eastern China (the coastal wetlands in Region IV), and Southern China (Region V), the climate-induced increase in CH_4 fluxes from inland and coastal wetlands will be lower.

However, if precipitation remains unchanged, warming conditions will be accompanied by increased drought and rising sea levels (Lin et al., 2011), which will produce a negative impact on regional CH_4 emissions. In the inland wetlands, such as the marshlands of the Sanjiang Plain (Region I) and the peatlands of the Qinghai Tibetan Plateau (Region II), drought conditions will increase evapotranspiration, decrease the anti-interference ability of wetlands, speed up wetland degradation (Liu et al., 2001), and ultimately decrease CH_4 fluxes and regional CH_4 emissions in the future. For the lakes and rivers, drought is expected to reduce the lake areas (Yu et al., 2004) and decrease regional CH_4 emissions in northeastern China (Region I) and Inner Mongolia. Although short-term expansion in the lakes may occur because of glacial melting over the western plateau of China (Region II and western Region III), water shortages will result in the long-term disappearance of the lakes (Shen et al., 2003a). Fortunately, precipitation is expected to increase, especially in northern China (Region I, Region III and the inland wetlands in Region IV) and on the Qinghai

Tibetan Plateau (Region IV) (Ding and Ren, 2007), which may offset the negative impact on CH_4 emissions from the inland wetlands and lakes by the imminent drought conditions. For the coastal wetlands, rising sea levels will reduce the area of coastal wetlands by inundation. Consider the Jiangsu Province in eastern China (Region IV) as an example, where 396, 617 and 1390 km^2 is expected to be lost in the next 30, 50 and 100 years, respectively (Li et al., 2006b). Moreover, rising sea levels will increase the invasion of salt water to estuarine wetlands (Shen et al., 2003b; Hu et al., 2003; Huang and Xie, 2000), which will reduce CH_4 fluxes due to the higher salinity.

The Chinese government announced the China National Wetland Conservation Action Plan (NWCP) in 2000 and approved it in 2003 (Editorial Committee, 2009). The NWCP had a set of ambitious goals, including the establishment of 713 wetland reserves with more than 90% of natural wetlands effectively protected by 2030, the restoration of 1.4×10^9 ha of natural wetlands, and the establishment of 53 national pilot zones for wetland protection and prudent use. Previous studies have shown that wetland restoration increases CH_4 emissions (Waddington et al., 2009; Jauhiainen et al., 2008; Basiliko et al., 2007; Bortoluzzi et al., 2006; Roulet, 2000). According to this research, NWCP may decelerate wetland loss and increase CH_4 emissions by the restoration of natural wetlands. However, in China, the present research on wetland restoration has mostly focused on water (e.g., Wang et al., 2005; Chen et al., 2006), soil (e.g., Tian et al., 2004) and plants (e.g., Pan et al., 2004). The balance of greenhouse gases and their role in global climate regulation were neglected by both the government and researchers. To assess a more comprehensive ecological effect of wetland restoration, the monitoring of the greenhouse gases from reserved natural wetlands should also be added to the NWCP project.

4.4 Present state and research gaps in CH_4 modeling

With the observation of atmospheric CH_4 concentrations, Zhang et al. (2013) provided an estimation of 4.76 Tg CH_4 emissions (Table 2) from the wetlands of China, which is twice the estimation in this study. Although the application of the top-down methods faces challenges from the spatially sparse observations of the atmospheric CH_4, the existence of large differences among studies via multiple approaches indicates that we still have huge gaps between our knowledge and the true CH_4 emissions from natural wetlands.

Matthews and Fung (1987) began the modeling of the wetland methane emission by using vegetation, soil and fractional inundation maps, which led to process based modeling of CH_4 production, oxidation and transport (Cao et al., 1996; Walter et al., 1996; Potter et al., 1997; Zhang et al., 2002). Recently, the WETCHIMP project (Wetland CH_4 Inter-comparison of Models Project) evaluated the present ability to simulated large-scale CH_4 emissions from wetlands. In this study, the $CH4MOD_{wetland}$ and WETCHIMP models, e.g., CLM4Me (Rieley et al., 2011), LPJ-WhyMe (Wania et al., 2010), DLEM (Tian et al., 2010; 2015; Xu et al., 2010), ORCHIDEE (Krinner et al., 2005), SDGVM (Woodward et al., 1995; Beerling and Woodward, 2001), are all process-based models used for simulating CH_4 production, oxidation and transport processes in wetlands. In most of the models, the methane production rates are determined by the availability of methanogenic substrates and the influence of environmental factors, including soil temperature, soil texture, redox potential and pH. In $CH4MOD_{wetland}$, the methanogenic substrates include root exudates, plant litter and soil organic matter, which is a mechanism advantage over the DLEM, CLM4Me and ORCHIDEE model. DLEM only considers CH_4 production from dissolved organic carbon (DOC). In CLM4Me, the CH_4 production is related to the heterotrophic respiration from soil and litter. ORCHIDEE uses a fraction of the most labile "Litter + soil C" pool. The soil redox potential, dropping after flooding and rising when drying up, is a key environmental factor that regulates the production of CH_4. Wania et al. (2010) considered that the the soil redox as well as pH should be excluded because they are poorly characterized and LPJ-WhyMe, therefore, does not consider the influences of the redox potential and pH. However, Riley et al. (2011) incorporated the impacts of pH and the redox potential into the CLM4Me model. In $CH4MOD_{wetland}$, we considered the influence of redox potential but not pH because the impacts of soil pH on the activity of methanogenics are not so influential and direct as the redox potential. The $CH4MOD_{wetland}$ model assigned a fixed proportion of CH_4 oxidation during transport through the plant and by diffusion, which was similar to the method used in the DLEM, SDGVM and ORCHIDEE models.

In addition to the fallacy in the model mechanism, the poor availability of the model inputs also accounts for a large proportion of the uncertainty in regional estimations. The first important reason is the spatial variability in the water table depth. The TOPMODEL-based scheme (Beven and Kirkby, 1979) has been used to model regional water table depth in natural wetlands in both the WETCHIMP project as well as this study. It is based on the topographic wetness index (TWI) and assumes that water tables follow topographic holds (Haitjema and Mitchell-Bruker, 2005). However, the TWI is static and relies on the assumption that the local slope is an adequate proxy for the effective downslope hydraulic gradient, which is not necessarily true in low-relief terrains (Grabs, et al., 2009). Therefore, this algorithm is less suitable in flat areas and will induce uncertainties in the simulated water table depth. Moreover, the HYDRO1k global values for the TWI provided by the USGS in 2000 (USGS, 2000) are the most commonly used data for the TOPMODEL method. However, the limited resolution and quality of the data can induce uncertainties, especially in tropical wetlands (Marthews et al., 2015; Collins et al., 2011). More accurate descriptions of the hydrology process and higher-resolution datasets are needed to reduce the error in the simulated water table depth.

The change in wetland area is another key factor that must be considered seriously. Unfortunately, time series data on wetland changes at regional scales are often unavailable. Popular methods for defining the extent of wetlands include using “Prescribed constant wetland extents” and the “Hydrological model” (Melton et al., 2013; Wania et al., 2013). Using different methods, Melton et al. (2013) reported that the estimate of global wetland area ranged from 7.1×10^6 to 26.9×10^6 km^2. The TOPMODEL scheme was extensively used to predict wetland distribution dynamics (Kleinen et al., 2012; Stocker et al., 2014; Melton et al., 2013). It is true that the “Hydrological model” can reflect the annual or seasonal variations of the wetland area, which were considered to be the dominant cause of the seasonal variations of regional CH_4 emissions (Ringeval et al., 2010). However, this method is not suitable for simulating the historical wetland area in China. The reason is because the simulated wetland extent will not be sensitive to the influences of anthropogenic changes to the land surface (Wania et al., 2013), which could lead to an overestimate of the wetland area.

In China, the annual marshland area had been temporally interpolated using a negative correlation between the Chinese population and the marshland area of 1950 and 2000 (Liu and Tian, 2010; Xu and Tian, 2012). However, this relationship inevitably resulted in large uncertainties because human activity was, though important, not the only driving factor in wetland changes. For example, drought induced by climate warming is also the main reason for the wetland loss on the

Tibetan Plateau (Niu et al., 2012). Using this method, the marshland loss considered by Xu and Tian (2012) was only half of that in this study. We used the wetland area retrieved from remotely sensed data and the national land use data to deduce the wetland area of different times (see materials and methods). However, the "Prescribed constant wetland extents" lacked the seasonal variations of the wetland extent. Furthermore, the influence of human disturbance should also be considered to improve the performance of the "Hydrological model" (Melton et al., 2013; Wania et al., 2013) to more accurately delineate variations of the wetland extents at different temporal scales.

The vegetation parameters in the CH_4 models usually refer to the production of labile organic compounds from gross primary production (GPP) and the transport of CH_4 to the atmosphere via plant stems and leaves. These vegetation parameters are different among plant species but are usually unified in regional simulations. The differences in vegetation effectively influence the CH_4 fluxes as proven by King and Reeburgh (2002), documenting the relation between CH_4 and net primary production (NPP) in tundra vegetation. Verville et al. (1998) and Busch and Lösch (1999) have also shown a difference in the plant transport of CH_4 through aerenchymous tissues between vegetation types. In this study, other herbaceous plant species excluding *Carex* and *Phragmites* were neglected. This is not only due to the lack in measurement data but also because the distribution of these plant species were not available.

The limited resolution in the model upscaling may also produce uncertainties in the regional estimate due to the high spatial heterogeneity of the wetland methane fluxes. The substantially intra-grid heterogeneity in the water table depth and the NPP at a resolution of 0.5° might raise the representative error. We compared the simulated and observed CH_4 fluxes in Figures S1 and S2, which showed that the averaged input data yielded a significant estimation bias due to the admittance of the heterogeneity details and the non-linearity of the model mechanism.

5. Summary remarks

Climate warming has increased CH_4 fluxes at a rate of 0.52 g m^{-2} per decade from 1950 to 2010. However, during the same period, an estimated 2.35 Tg (1.91—2.81 Tg) of CH_4 reduction in Chinese wetlands occurred, which was mainly due to the extensive wetland loss from 35.6 million ha to 18.6 million ha. On a national scale, northeastern China experienced a large temperature increase which has resulted in the highest rate of a CH_4 flux increment of 0.67 g m^{-2} per decade. However, serious wetland loss has made northeastern China the largest contributor to the national CH_4 decrease, accounting for 70% of the total CH_4 reduction. The Qinghai-Tibetan Plateau had the lowest CH_4 reduction, which was approximately 8% of the reduction in northeastern China. Among the reduction, the inland wetlands, lakes/rivers and the coastal wetlands accounted for 81%, 11% and 8%, respectively, of the national CH_4 emission reduction.

Author contribution

T. Li, W. Zhang, T. Vesala. and M. Raivonen designed the research; T. Li, Q. Zhang and G. Wang performed the CH_4 modeling; Y. Lu performed the TEM modeling; Z. Niu prepared the time series of the wetland area; T. Li and W. Zhang prepare the manuscript with contribution from all coauthors.

Acknowledgements

This work was supported by the National Natural Science Foundation of China (Grant No. 31000234, 41321064 and 41175132), the Chinese Academy of Sciences (CAS) strategic pilot technology special funds (Grant No. XDA05020204), the Academy of Finland Center of Excellence (Grants No. 1118615 and 272041), ICOS 271878, ICOS-Finland 281255, ICOS-ERIC 281250, Academy Professor projects (1284701 and 1282842) and the Nordic Centre of Excellence DEFROST. We are grateful to Professor Yao Huang in the Institute of Botany, CAS to provide the valuable recommendations to the study. We would also like to thank the Pan-Eurasian Experiment (PEEX) for providing the data for model calibration and validation.

References

An, S. Q., Li, H. B., Guan, B. H., Zhou, C. F., Wang, Z. S., Deng, Z. F., Zhi, Y. B., Liu, Y. L., Xu, C., Fang, S. B., Jiang, J. H., and Li, H. L.: China’s natural wetlands: past problems, current status, and future challenges, Ambio, 36, 335-342, 2007.

Antonov, J. I., Seidov, D., Boyer, T. P., Locarnini, R. A., Mishonov, A. V., Garcia, H. E., Baranova, O. K., Zweng, M. M. and Johnson, D. R.: World Ocean Atlas 2009 Vol. 2, Salinity, in: NOAA Atlas NESDIS 69, edited by: Levitus, S., US

Government Printing Office, Washington, D.C., 1-184, 2010.

Atkinson, L. P. and Hall, J. R.: Methane distribution and production in the Georgia salt marsh, Estuarine Coastal Mar. Sci., 4, 677–686, 1976.

Bastviken, D., Cole, J., Pace, M., and Tranvik, L.: Methane emissions from lakes: Dependence of lake characteristics, two regional assessments, and a global estimate, Global Biogeochem. Cy., 18, GB4009, doi:10.1029/2004GB002238, 2004.

Bartlett, K. B., Harriss, R. C. and Sebacher, D. I.: Methane flux from coastal salt marshes, J. Geophys. Res., 90, 5710–5720, 1985.

Bartlett, K. B., Bartlett, D. S., Harriss, R. C. and Sebacher, D. I.: Methane emissions along a salt marsh salinity gradient, Biogeochemistry, 4, 183–202, 1987.

Basiliko, N., Blodau, C., Roehm,C., Bengtson, P. and Moore, T. R.: Regulation of decomposition and methane dynamics across natural, commercially mined, and restored northern peatlands, Ecosystems, 10, 1148–65, 2007.

Beerling, D. J. and Woodward, F. I.: Vegetation and the terrestrial carbon cycle: Modelling the first 400 Million Years, Cambridge University Press, Cambridge, 2001.

Berrittella, C., and Huissteden, J. V.: Uncertainties in modelling CH_4 emissions from northern wetlands in glacial climates: the role of vegetation parameters, Clim. Past, 7, 1075-1087, 2011.

Beven, K. J. and Kirkby, M. J.: A physically based, variable contributing area model of basin hydrology, Hydrolog. Sci. Bull., 24, 43-69, 1979.

Belward, A. S., Estes, J. E. and Kline, K. D.: The IGBP-DIS global 1-km land-cover data set DISCover: A project overview, Photogramm. Eng. Rem. S., 65, 1013-1020, 1999.

Bohn, T. J., Lettenmaier, D. P., Sathulur, K., Bowling, L. C., Podest, E., McDonald, K. C. and Friborg, T.: Methane emissions from western Siberian wetlands: heterogeneity and sensitivity to climate change, Environ. Res. Lett., 2, 045015 doi:10.1088/1748-9326/2/4/045015, 2007.

Bohn, T. J., Melton, J. R., Ito, A., Kleinen, T., Spahni, R., Stocker, B. D., Zhang, B., Zhu, X., Schroeder, R., Glagolev, M. V., Maksyutov, S., Brovkin, V., Chen, G., Denisov, N. S., Eliseev, A. V., Gallego-Sala, A., McDonald, K. C., Rawlins, M. A., Riley, W. J., Subin, Z. M., Tian, H., Zhuang, Q., and Kaplan, J. O.: WETCHIMP-WSL: intercomparison of wetland methane emissions models over

West Siberia, Biogeosciences, 12, 3321-3349, 2015.

Bortoluzzi, E., Epron, D., Siegenthaler, A., Gilbert, D. and Buttler, A.: Carbon balance of a European mountain bog at contrasting stages of regeneration, New Phytol., 172, 708–18, 2006.

Bousquet, P., Cialis, P., Miller, J. B., Dlugokencky, E. J., Hauglustaine, D. A., Prigent, C., van der Werf, G. R., Peylin, P., Brunke, E.-G., Carouge, C., Langenfelds, R. L., Lathi`ere, J., Papa, F., Ramonet, M., Schmidt, M., Steele, L. P., Tyler, S. C., and White, J.: Contribution of anthropogenic and natural sources to atmospheric methane variability, Nature, 443, 439-443, doi:10.1038/nature05132, 2006.

Bush, J. and L ̈osch, R.: The Gas Exchange of Carex Species from Eutrophic Wetlands and its Dependence on Microclimatic and Soil Wetness Conditions, Phys. Chem. Earth B, 24, 117–120, 1999.

Cai, Z. C.: Greenhouse gas budget for terrestrial ecosystems in China, Sci. China Earth Sci., 55, 173-182, 2012.

Cao, M. K., Marshall, S., and Gregson, K.: Global carbon exchange and methane emissions from natural wetlands: Application of a process-based model, J. Geophys. Res.-Atmos., 101, 14399-14414, 1996.

Chen, H., Yao, S., Wu, N., Wang, Y., Luo, P., Tian, J., Gao, Y., and Sun, G.: Determinants influencing seasonal variations of methane emissions from alpine wetlands in Zoige Plateau and their implications. J. Geophys. Res., 113: D12303, doi:10.1029/2006JD008072, 2008.

Chen, H., Wu, Y., Yuan, X., Gao, Y., Wu, N. and Zhu, D.: Methane emissions from newly created marshes in the drawdown area of the Three Gorges Reservoir, J. Geophys. Res., 114**,** D18301, doi:10.1029/2009JD012410, 2009.

Chen, H., Zhu, Q., Peng, C. H., Wu, N., Wang, Y. F., Fang, X. Q., Jiang, H., Xiang, W. H., Chang, X., Deng, X. W. and Yu G. R.: Methane emissions from rice paddies natural wetlands, lakes in China: synthesis new estimate, Glob. Change Biol., 19, 19-32, 2013.

Chen, K. N., Bao, X. M., Shi, L. X., Chen, W. M., Lan, C. J., Xu, H., Hu, H. Y.: Ecological restoration engineering in Lake Wuli, Lake Taihu: a large enclosure experiment, J. Lake Sci., 18, 139-149, 2006. (in Chinese with English abstract)

Christensen, T. and Cox, P.: Response of methane emission from arctic tundra to climate change: results from a model simulation, Geophys. Res. Lett., 31, L04501, doi:10.1029/2003GL018680, 1995.

Christensen, T. R., Ekberg, A., Ström, L., Mastepanov, M., Panikov, N., Öquist, M., Svensson, B. H., Nykänen, H., Martikainen, P. J. and Oskarsson, H.: Factors controlling large scale variations in methane emissions from wetlands, Geophys. Res. Lett., 30, 1414, doi:10.1029/2002GL016848, 2003.

Collins, W., Bellouin, N., Doutriaux-Boucher, M., Gedney, N., Halloran, P., Hinton, T., Hughes, J., Jones, C. D., Joshi, M., Liddicoat, S., Martin, G., O'Connor, F., Rae, J., Senior, C., Sitch, S., Totterdell, I., Wiltshire, A. and Woodward, S.: Development and evaluation of an Earth-system model-HadGEM2, Geosci. Model Dev., 4, 1051-1075, 2011.

Cramer, W., Kicklighter, D. W., Bondeau, A., Moore Iii, B., Churkina, G., Nemry, B., Ruimy, A., Schloss, A. L., and The Participants of the Potsdam NPP Model Intercomparison: Comparing global models of terrestrial net primary productivity (NPP): overview and key results, Glob. Change Biol., 5, 1-15, 1999.

Davidson, N. C.: How much wetland has the world lost? Long-term and recent trends in global wetland area, Mar. Freshwater Res., 65, 934-941, 2014.

Denman, K. L., Brasseur, G., Chidthaisong, A., Ciais, P., Cox, P. M., Dickinson, R. E., Hauglustaine, D., Heinze, C., Holland, E., Jacob, D., Lohmann, U., Ramachandran, S., da Silva Dias, P. L., Wofsy, S. C., and Zhang, X.: Couplings between changes in the climate system and biogeochemistry, in: Climate Change 2007: The Physical Science Basis. Contribution of Working Group I to the Fourth Assessment Report of the Intergovernmanetal Panel on Climate Change, edited by: Solomon, S., Qin, D., Manning, M., Chen, Z., Marquis, M., Averyt, K. B., Tignor, M. and Miller, H. L., Cambridge University Press, Cambridge, 539-544, 2007.

Ding, W., X., Cai, Z. and Wang, D.: Preliminary budget of methane emissions from natural wetlands in China, Atmos. Environ., 38, 751-759, 2004.

Ding, W. X. and Cai, Z. C.: Methane emission from natural wetlands in China: summary of years 1995-2004 studies, Pedosphere, 17, 475-486, 2007.

Ding, Y. H. and Ren, G. Y.: Climate change in China and its future trend, in: National assessment report of climate change, edited by: editing committee of national assessment report of climate change, Science Press, China, 130-161, 2007. (in Chinese with English abstract)

Du, X., and Chen, W.: Methodology for managing the effect of uncertainty in simulation-based design, AIAA J., 38, 1471-1478, 2000.

Duan, X. N., Wang, X. K., Mu, Y. J. and Ouyang, Z. Y.: Seasonal and diurnal variations in methane emissions from Wuliangsu Lake in arid regions of China, Atmos. Environ., 39, 4479-4487, 2005.

Editorial Committee: China wetlands encyclopedia, Beijing Science and Technology Press, Beijing, 2009. (in Chinese)

Fan, Y. and van den Dool, H.: Climate prediction center global monthly soil moisture data set at 0.5° resolution for 1948 to present, J. Geophys. Res., 109, D10102, doi:10.1029/2003JD004345, 2004.

FAO/IIASA/ISRIC/ISS-CAS/JRC: Harmonized World Soil Database, version 1.0, FAO, Rome,Italy and IIASA, Laxenburg, Austria, 2008.

FAO/IIASA/ISRIC/ISSCAS/JRC: Harmonized World Soil Database, version 1.2, FAO and IIASA, Rome, Italy and Laxenburg, Austria, 2012.

Forster, P., Ramaswamy, V., Artaxo, P., Berntsen, T., Betts, R., Fahey, D., Haywood, J., Lean, J., Lowe, D., Myhre, G., Nganga, J., Prinn, R., Raga, G., Schulz, M. and Van Dorland, R.: Changes in atmospheric constituents and in radiative forcing, in: Climate Change 2007: The Physical Science Basis. Contribution of Working Group I to the Fourth Assessment Report of the Intergovernmental Panel on Climate Change, edited by: Solomon, S., Qin, D., Manning, M., Chen, Z., Marquis, M., Averyt, K. B., Tignor, M. and Miller, H. L., Cambridge University Press, Cambridge, 131-243, 2007.

Fung, I., John, J., Lerner, J., Matthews, E., Prather, M., Steele, L., and Fraser, P.: Three-dimensional model synthesis of the global methane cycle, J. Geophys. Res., 96, D7, 13033-13065, 1991.

Gill, R. and Jackson, R. B.: Global Distribution of Root Turnover in Terrestrial Ecosystems, Oak Ridge National Laboratory Distributed Active Archive Center, Oak Ridge, Tennessee, U.S.A. doi:10.3334/ORNLDAAC/661, 2003.

Giltrap, D. L., Li, C. C., and Saggar, S.: DNDC: A process-based model of greenhouse gas fluxes from agricultural soils, Agr. Ecosyst. Environ., 136, 292-300, 2010.

Grabs, T., Seibert, J., Bishop, K. and Laudon, H.: Modeling spatial patterns of saturated areas: A comparison of the topographic wetness index and a dynamic distributed model, J. Hydrol., 373, 15-23, 2009.

Haitjema, H. M. and Mitchell-Bruker, S.: Are water tables a subdued replica of the topography? Ground Water, 43, 781-786, 2005.

Harris, I., Jones, P. D., Osborn, T. J. and Lister, D. H.: Updated high-resolution grids of monthly climatic observations-the CRU TS3.10 Dataset, Int. J. Climatol., 1, doi: 10.10, 2014.

Hein, R., Crutzen, P. J., and Heimann, M.: An inverse modeling approach to investigate the global atmospheric methane cycle, Global Biogeochem. Cy., 11, 43-76, 1997.

Hirota, M., Tang, Y., Hu, Q., Hirata, S., Kato, T., Mo, W., Gao, G. M. and Marikoe, S.: Methane emissions from different vegetation zones in a Qinghai-Tibetan Plateau wetland, Soil Biol. Biochem., 36, 737–748, 2004.

Huang, G. H., Li, X. Z., Hu, Y. M., Shi, Y. and Xiao, D. N.: Methane emission from a natural wetland of northern China, J. Environ. Sci. Heal. A, 40, 1227–1238, 2005.

Huang, Y., Sass, R. L. and Fisher, F. M.: A semi-empirical model of methane emission from flooded rice paddy soils, Glob. Change Biol., 4, 247–268, 1998.

Huang, Y., Zhang, W., Zheng, X., Li, J. and Yu, Y.: Modeling methane emission from rice paddies with various agricultural practices, J. Geophys. Res., 109, D08113, doi: 10.1029/2003JD004401, 2004.

Huang, Y., Zhang, W., Zheng, X., Han, S. and Yu, Y.: Estimates of methane emissions from Chinese rice paddies by linking a model to GIS database, Acta Ecologica Sinica, 26, 980–987, 2006.

Huang, Y., Sun, W., Zhang, W., Yu, Y. Q., Su, Y. H. and Song, C. C. Marshland conversion to cropland in northeast China from 1950 to 2000 reduced the greenhouse effect, Glob. Change Biol., 16, 680-695, 2010.

Huang, Z. G. and Xie, X. D.: Change of the sea level and its effect and countermeasures, Guangdong science and Technology Press, China, 2000. (in Chinese)

Hu, S., Zhu, J. R., Fu, D. J. and Wu, H.: Estuarine circulation and saltwater intrusion II: impacts of river discharge and rise of sea level, Journal of Ocean University of Qingdao, 33, 337-342, 2003. (in Chinese with English abstract)

IPCC: Emission Scenarios: A Special Report of Workgroup III of IPCC. Cambridge University Press, UK, 2000.

IPCC: Climate Change 2007: The Physical Science Basis. Contribution of Working Group I to the Fourth Assessment Report of the Intergovernmental Panel on Climate Change, edited by: Solomon, S., Qin, D., Manning, M., Chen, Z., Marquis, M., Averyt, K. B., Tignor, M. and Miller, H. L.). Cambridge University Press, Cambridge, 2007.

IPCC: Climate Change 2013: The Physical Science Basis. Contribution of Working Group I to the Fifth Assessment Report of the Intergovernmental Panel on Climate Change, edited by: Stocker, T. F., Qin, D., Plattner, G. K., Tignor, M., Allen, S. K., Boschung, J., Nauels, A., Xia, Y., Bex, V. and Midgley, P. M., Cambridge University Press, Cambridge, 2013.

Jin, H. J., Wu, J., Cheng, G. D., Tomoko, N. and Sun, G. Y.: Methane emissions from wetlands on the Qinghai-Tibet Plateau, Chinese Sci. Bull., 44, 2282-2286, 1999.

Jauhiainen, J., Limin, S., Silvennoinen, H. and Vasander, H.: Carbon dioxide and methane fluxes in drained tropical peat before and after hydrological restoration, Ecology, 89, 3503–14, 2008.

Kesik, M., Ambus, P., Baritz, R., Brüggemann, N., Butterbach-Bahl, K., Damm, M., Duyzer, J., Horváth, L., Kiese, R., Kitzler, B., Leip, A., Li, C., Pihlatie, M., Pilegaard, K., Seufert, S., Simpson, D., Skiba, U., Smiatek, G., Vesala, T., and Zechmeister-Boltenstern, S.: Inventories of N_2O and NO emissions from European forest soils, Biogeosciences, 2, 353-375, doi:10.5194/bg-2-353-2005, 2005.

Khalil, M. A. K., Shearer, M. J. and Rasmussen, R. A.: Methane sources in China: historical and current emissions, Chemosphere, 26, 127-142, 1993.

King, G. M. and Wiebe, W. J.: Methane release from soils of a Georgia salt marsh, Geochimi. Cosmochim. Ac., 42, 343–348, 1978.

King, J. Y. and Reeburgh, W. S.: A pulse-labeling experiment to determine the contribution of recent plant photosynthates to net methane emission in arctic wet sedge tundra, Soil Biol. Biochem., 34, 173-180, 2002.

Kleinen, T., Brovkin, V. and Schuldt, R. J.: A dynamic model of wetland extent and peat accumulation: results for the Holocene, Biogeosciences, 9, 235-248, 2012.

Krinner, G., Viovy, N., de Noblet-Ducoudre, N., Ogee, J., Polcher, J., Friedlingstein, P., Ciais, P., Sitch, S., and Prentice, I. C.: A dynamic global vegetation model for studies of the coupled atmosphere-biosphere system, Global Biogeochem. Cy., 19, 941–962, 2005.

Lang, H. Q. and Zu, W. C.: Marshland in Chinese, Shandong Science and Technology Press, China, 1983. (in Chinese)

Li, C. C., Narayanan, V. and Harriss, R. C.: Model estimates of nitrous oxide emissions from agricultural lands in the United States, Global Biogeochem. Cy., 10, 297-306, 1996.

Li, C. C., Arvin, M., Reiner, W., Cai, Z. C., Zheng, X. H., Huang, Y., Haruo, T., Jariya, B., and Rhoda, L.: Modeling greenhouse gas emissions from rice‑based production systems: Sensitivity and upscaling. Global Biogeochem. Cy., 18, GB1043, doi:10.1029/2003GB002045, 2004.

Li, C., Salas, W., DeAngelo, B., and Rose, S.: Assessing alternatives for mitigating net greenhouse gas emissions and increasing yields from rice production in China over the next twenty years, J. Environ. Qual., 35, 1554-1565, 2006a.

Li, J. L., Wang, Y. H., Zhang, R. S., Qi, D. L. and Zhang, D. F.: Disaster effects of sea level rise - a case of Jiangsu coastal low land, Sci. Geograph. Sinica, 26, 87-93, 2006b. (in Chinese with English abstract)

Li, T., Huang, Y., Zhang, W. and Song, C.: CH4MOD$_{\text{wetland}}$: A biogeophysical model for simulating CH_4 emissions from natural wetland, Ecol. Model., 221, 666-680, 2010.

Li, T., Huang, Y., Zhang, W. and Yu, Y.: Methane emissions associated with the conversion of marshland to cropland and climate change on the Sanjiang Plain of northeast China from 1950 to 2100, Biogeosciences, 9, 1-17, 2012.

Lin, E. D., Wu, S. H. and Luo, Y.: Climate change impacts and adaptation, in: The second national assessment report of climate change, edited by: editing committee of the second national assessment report of climate change, Science Press, China, 195-339, 2011. (in Chinese with English abstract)

Liu, M. and Tian, H.: China's land cover and land use change from 1700 to 2005: Estimations from high-resolution satellite data and historical archives, Global Biogeochem. Cy., 24, GB3003, doi:10.1029/2009GB003687, 2010.

Liu, X. T. and Ma, X. H.: Influence of large scale reclamation on natural environment and regional environmental protection in the Sanjiang Plain, Sci. Geograph. Sinica, 20, 14-19, 2000. (in Chinese with English abstract)

Liu, Z. Q., Liu, H. Y. and Lv, X. G.: Ecological fragility of wetlands in Sanjiang Plain, Chinese J. Appl. Ecol., 12, 241-244, 2001. (in Chinese with English abstract)

Loveland, T. R., Brown, J. F., Ohlen, D. O., Zhu, Z., Yang, L., Merchant, J. W. and Reed, B. C.: Development of a global land cover characteristics database and IGBP DISCover from 1 km AVHRR data, Int. J. Remote Sens., 21, 1303-1330, 2000.

Lu, X. and Zhuang, Q.: Modeling methane emissions from the Alaskan Yukon River basin, 1986-2005, by coupling a larg-scale hydrological model and a process-based methane model, J. Geophys. Res., 117, G02010, doi:10.1029/2011JG001843, 2012.

Magenheimer, J. F., Moore, T. R., Chmura, G. L. and Daoust, R. J.: Methane and carbon dioxide flux from a macrotidal salt marsh, Bay of Fundy, New Brunswick Canada, Estuaries, 19, 139–145, 1996.

Marthews, T., Dadson, S., Lehner, B., Abele1, S. and Gedney, N.: High-resolution global topographic index values for use in large-scale hydrological modeling, Hydrol. Earth Syst. Sc., 19, 91-104, 2015.

Matthews, E. and Fung, I. Y.: Methane emission from natural wetlands: Global distribution, area, and environmental characteris characteristics of sources, Global Biogeochem. Cy., 1, 61–86, 1987.

McGuire, A. D., Melillo, J. M., Joyce, L. A., Kicklighter, D. W., Grace, A. L., Moore III, B. and Vorosmarty, C. J.: Interactions between carbon and nitrogen dynamics in estimating net primary productivity for potential vegetation in North America, Global Biogeochem. Cy., 6, 101-124, 1992.

Melillo, J. M., Mcguire, A. D., Kicklighter, D. W., Moore, B., Vorosmarty, C. J. and Schloss, A. L.: Global climate change and terrestrial net primary production, Nature, 363, 234-240, 1993.

Melton, J., Wania, R., Hodson, E. L., Poulter, B., Ringeval, B., Spahni, R., ,Bohn, T., Avis, C. A.,Beerling, D. J., Chen, G., Eliseev, A. V., Denisov, S. N., Hopcroft, P. O., Lettenmaier, D. P., Riley, W. J., Singarayer, J. S., Subin, Z. M.,Tian, H., Zurcher, S., Brovkin, V., van Bodegom, P. M., Kleinen, T., Yu, Z. C.,and Kaplan : Present state of global wetland extent and wetland methane modelling: conclusions from a model intercomparison project (WETCHIMP), Biogeosciences 10: 753-788, 2013.

Montzka, S. A., Dlugokencky, E. J., and Butler, J. H.: Non-CO_2 greenhouse gases and climate change, Nature, 476, 43-50, 2011.

Moser, M., Prentice, C. and Frazier, S.: A global overview of wetland loss and degradation. Proceedings to the 6th Meeting of the Conference of Contracting Parties of the Ramsar Convention, Brisbane, Australia, Vol. 10/12B, 21-31, March 1996.

Niu, Z. G., Zhang, H. Y., Wang, X. W., Yao W. B., Zhou, D. M., Zhao, K. Y., Zhao, H., Li, N. N., Huang, H. B., Li, C. C., Yang, J., Liu, C. X., Liu, S., Wang, L., Li, Z., Yang, Z. Z., Qiao, F., Zheng, Y. M., Chen, Y. L., Sheng, Y. W., Gao X. H., Zhu, W. H., Wang, W. Q., Wang, H., Weng, Y. L., Zhuang, D. F., Liu, J. Y., Luo, Z. C., Cheng, X., Guo, Z. Q. and Gong, P.: Mapping wetland changes in China between 1978 and 2008, Chinese Sci. Bull., 57, 2813-2823, 2012.

Nisbet, E. G., Dlugokencky, E. J. and Bousquet, P.: Methane on the rise-again. Science, 343, 493-495, 2014.

Pan, J. Z., Li, W. C., Chen, K. N.: A study on the environmental effect in the zone of restoration of aquatic plants covered at the northeast in Dianchi Lake: I. the effect of controlling of alga blooming, J. Lake, Sci., 16, 141-148. (in Chinese with English abstract)

Poffenbarger, H. J., Needelman, B. A. and Megonigal, J. P.: Salinity influence on methane emissions from tidal marshes, Wetlands, 31, 831–842, 2011.

Potter, C.: An ecosystem simulation model for methane production and emission from wetlands, Global Biogeochem. Cy., 11, 495– 506, 1997.

Potter, C., Klooster, S., Hiatt, S., Fladeland, M., Genovese, V. and Gross, P.: Methane emissions from natural wetlands in the United States: satellite-derived estimation based on ecosystem carbon cycling, Earth Interact., 10, 1-12, 2006.

Ramsar, Iran: Ramsar convention of wetlands of international importance, especially as waterfowl habitat, Ramsar, Iran, 1971.

Revenga, C., Brunner, J., Henninger, N., Kassem, K. and Payne, R.: Pilot analysis of global ecosystems: Freshwater systems, World Resources Institute, Washington, DC, 2000.

Ringeval, B., de Noblet‐Ducoudré, N., Ciais, P., Bousquet, P., Prigent, C., Papa, F., and Rossow, W. B.: An attempt to quantify the impact of changes in wetland extent on methane emissions on the seasonal and interannual time scales, Global Biogeochem. Cy., 24, GB2003, doi:10.1029/2008GB003354, 2010.

Riley, W., Subin, Z. M., Lawrence, D. M., Swenson, S. C., Torn, M. S., Meng, L., Mahowald, N. M., and Hess, P.: Barriers to predicting changes in global terrestrial methane fluxes: analyses using CLM4Me, a methane biogeochemistry model integrated in CESM, Biogeosciences, 8(7), 1925-1953, 2011.

Roulet, N. T.: Peatlands, carbon storage, greenhouse gases, and the Kyoto Protocol:

prospects and significance for Canada, Wetlands, 20, 605–15, 2000.

Shindell, D. T., Walter, B. P. and Faluvegi, G.: Impacts of climate change on methane emissions from wetlands, Geophys. Res. Lett., 31, L21202, doi:10.1029/2004GL021009, 2004.

Shindell, D. T., Faluvegi, G., Koch, D. M., Schmidt, G. A., Unger, N. and Bauer, S. E.: Improved attribution of climate forcing to emissions, Science, 326, 716-718, 2009.

Shen, Y. P., Liu, S. Y., Ding, Y. J. and Wang, S. D.: Glacier mass balance change in Tailanhe river watersheds on the south slope of the Tianshan Mountains and its impact on water resources, J. Glaci. Geocry., 25, 124-129, 2003a. (in Chinese with English abstract)

Shen, H. T., Mao, Z. C. and Zhu, J. R.: Salt water intrusion in ChangJiang Estuary, China Ocean Press, China, 2003b. (in Chinese with English abstract)

Song, C. C., Zhang, J. B., Wang, Y. Y., Wang, Y. S. and Zhao, Z. C.: Emission of CO_2, CH_4 and N_2O from freshwater marsh in northeast of China, J. Environ. Manage., 40, 6879–6885, 2007.

Stocker, B. D., Spahni, R., and Joos, F.: DYPTOP: a costefficient TOPMODEL implementation to simulate sub-grid spatio-temporal dynamics of global wetlands and peatlands, Geosci. Model Dev., 7, 3089–3110, doi:10.5194/gmd-7-3089-2014, 2014.

Streets, D. G., Jiang, K., Hu, X., Sinton, J. E., Zhang, X.-Q., Xu, D., Jacobson, M. Z., and Hansen, J. E.: Recent reductions in China’s greenhouse gas emissions, Science, 294, 1835-1837, 2001.

Tian, H., Xu, X., Liu, M., Ren,W., Zhang, C., Chen, G., and Lu, C.: Spatial and temporal patterns of CH_4 and N_2O fluxes in terrestrial ecosystems of North America during 1979–2008: application of a global biogeochemistry model, Biogeosciences, 7, 2673–2694, doi:10.5194/bg-7-2673-2010, 2010.

Tian, H., Xu, X., Lu, C., Liu, M. L., Ren, W., Chen, G. S., Melillo, J. and Liu, J. Y.: Net exchanges of CO_2, CH_4, and N_2O between China’s terrestrial ecosystems and the atmosphere and their contributions to global climate warming, J. Geophys. Res., 116, G02011, doi:10.1029/2010JG001393, 2011.

Tian, H., Chen, G., Lu, C., Xu, X., Ren, W., Zhang, B., Banger, K., Tao, B., Pan, S., and Liu, M.: Global methane and nitrous oxide emissions from terrestrial ecosystems due to multiple environmental changes, Ecosyst. Health

Sustainability, 1, http://dx.doi.org/10.1890/EHS14-0015.1, 2015.

Tian, Y. B., Xiong, M. B., Song, G. Y.: Study on change of soil organic matter in the process of wetland ecological restoration in Ruoergai Plateau, Wetland Sci., 2, 88-93, 2004. (in Chinese with English abstract)

USGS: US Geological Survey: HYDRO1k Elevation derivative database, US Geological Survey Earth Resources Observation and Science (EROS) Center, Sioux Falls, South Dakota, 2000.

Verville, J. H., Hobbie, S. E., Chapin III, F. S., and Hooper, D. U.: Response of tundra CH_4 and CO_2 flux to manipulation of temperature and vegetation, Biogeochemistry, 41, 215–235, 1998.

Waddington, J. M., Plach, J., Cagampan, J. P., Lucchese, M. and Strack, M.: Reducing the carbon footprint of Canadian peat extraction and restoration, Ambio, 38, 194-200, 2009.

Walter, B. P., Heimann, M., Shannon, R. D., and White, J.: A process-based model to derive methane emissions from natural wetlands, Geophys. Res. Lett., 23, 3731–3734, 1996.

Wania, R., Ross, I., and Prentice, I. C.: Implementation and evaluation of a new methane model within a dynamic global vegetation model: LPJ-WHyMe v1. 3.1, Geosci. Model Dev. 3, 565-584, 2010.

Wania, R., Melton, J. R., Hodson, E. L., Poulter, B., Ringeval, B., Spahni, R., Bohn, T., Avis, C. A., Chen, G., Eliseev, A. V., Hopcroft, P. O., Riley, W. J., Subin, Z. M., Tian, H., van Bodegom, P. M., Kleinen, T., Yu, Z. C., Singarayer, J. S., Zürcher, S., Lettenmaier, D. P., Beerling, D. J., Denisov, S. N., Prigent, C., Papa, F., and Kaplan, J. O.: Present state of global wetland extent and wetland methane modelling: methodology of a model inter-comparison project (WETCHIMP), Geosci. Model Dev., 6, 617-641, 2013.

Wang, D., Kong, F. X., Liu, A. J., Tan, J. K., Cao, H. S.: Analysis of the influence of the ecological dredging to ecosystem Lake Wuli, Lake Taihu, J. Lake Sci., 17, 263-268, 2005. (in Chinese with English abstract)

Wang, M. X., Dai, A. G., Huang, J., Ren, L. X. and Shen, R. X.: Sources of methane in China: rice fields, agricultural waste treatment, cattle, coal mines, and other minor sources, Scientia Atmospherica Sinica, 17, 52-64, 1993. (in Chinese with English abstract)

Wang, S. M. and Dou, H. S.: Lakes in China, Science Press, Beijing, China, 1998. (in

Chinese)

Wang, Z., Wu, J., Madden, M., and Mao, D.: China's wetlands: conservation plans and policy impacts, Ambio, 41, 782-786, 2012a.

Wang, X. K., Lu, F. and Yang, L.: Methane emissions from China's natural wetlands: measurements, temporal variations and influencing factors, in: Recarbonization of the Biosphere, edited by: Lal, R., Lorenz, K., Hüttl, R. F., Schneider, B. U. and von Braun, J., Springer Netherlands, 99-125, 2012b.

Wei, D., Xu, R., Tenzin, T., Dai, D. X., Wang, Y. S., and Wang, Y. H.: Revisiting the role of CH_4 emissions from alpine wetlands on the Tibetan Plateau: evidence from two in situ measurements at 4758 and 4320 m above sea level. J. Geophys. Res.−Biogeosci., doi: 10.1002/2015JG002974, 2015.

Whalen, S. C.: Biogeochemistry of methane exchange between natural wetlands and the atmosphere, Environ. Eng. Sci., 22, 73-94, 2005.

Woodward, F. I., Smith, T. M., and Emanuel, W. R.: A global land primary productivity and phytogeography model, Global Biogeochem.Cy., 9, 471–490, 1995.

Xu, Q., Cai, L., Dong, Y. H.: Characteristics, types and management of the wetlands in China: Study on wetlands in China, edited by Chen Y. Y., Jilin Science and Technology Press, Changchun, Jilin, China, 1995, pp 24-33. (in Chinese)

Xu, X. F., Tian, H. Q., Zhang, C., Liu, M. L., Ren, W., Chen, G. S., Lu, C. Q., and Bruhwiler, L.: Attribution of spatial and temporal variations in terrestrial methane flux over North America, Biogeosciences, 7, 3637–3655, doi:10.5194/bg-7-3637-2010, 2010.

Xu, X. and Tian, H.: Methane exchange between marshland and the atmosphere over China during 1949-2008, Global Biogeochem. Cy., 26, GB2006, doi:10.1029/2010GB003946, 2012.

Yan, X., Akiyama, H., Yagi, K., and Akimoto, H.: Global estimations of the inventory and mitigation potential of methane emissions from rice cultivation conducted using the 2006 Intergovernmental Panel on Climate Change Guidelines, Global Biogeochem. Cy., 23, GB2002, doi:10.1029/2008GB003299, 2009.

Yang, W. Y., Song, C. C. and Zhang, J. B.: Dynamics of methane emissions from a freshwater marsh of northeast China, Sci. Total Environ., 371, 286-292, 2006.

Yang, H., Xie, P., Ni, L., and Flower, R. J.: Underestimation of CH_4 emission from freshwater lakes in China, Environ. Sci. Technol., 45, 4203-4204, 2011.

Yu, G., Lai, L. B. and Xu, B.: Preliminary Study on the responses of lake water from the western China to climate change in the future: Monte carlo analysis applied in GCM simulations and lake water changes, J. Lake Sci., 16, 193-202, 2004. (in Chinese with English abstract)

Zhang, J. B., Song, C. C., and Yang, W. Y.: Cold season CH_4, CO_2 and N_2O fluxes from freshwater marshes in northeast China, Chemosphere, 59(11), 1703-1705, 2005.

Zhang, Y., Li, C., Trettin, C. C., Li, H., and Sun, G.: An integrated model of soil, hydrology, and vegetation for carbon dynamics in wetland ecosystems, Global Biogeochem. Cy., 16(4): 1061-1078, 2002.

Zhang, W., Yu, Y., Huang, Y., Li, T. and Wang, P.: Modeling methane emissions from irrigated cultivation in China from 1960 to 2050, Glob. Change Biol., 17, 3511–3523, 2011.

Zhang, X., Jiang, H., Lu, X., Cheng, M., Zhang, X., Li, X. and Zhang, L.: Estimate of methane release from temperate natural wetlands using ENVISAT/SCIAMACHY data in China, Atmos. Environ., 69, 191-197, 2013.

Zhao, K. Y.: Mires in China, Science Press, Beijing,China, 1999. (in Chinese)

Zhao, K. Y., Liu, X. T.: Status qua and prospect of studies in wetlands, Study on wetlands in China, Jilin Science and Technology Press, Changchun, Jilin, China, 1995, pp 1-9. (in Chinese)

Zhuang, Q., Melillo, J., Kicklighter, D., Prinn, R. G., McGuire, A. D., Steudler, P. A., Felzer, B. S. and Hu, S.: Methane fluxes between terrestrial ecosystems and the atmosphere at northern high latitudes during the past century: A retrospective analysis with a process-based biogeochemistry model, Global Biogeochem. Cy., 18, GB3010, doi:10.102, 2004.

Zhuang, Q., Mellillo, J., Sarofim, M., Kicklighter, D. W., McGuire, A. D., Felzer, B. S., Sokolov, A., Prinn, R. G., Steudler, P. A. and Hu, S: CO_2 and CH_4 exchanges between land ecosystems and the atmosphere in northern high latitudes over the 21st century, Geophys. Res. Lett., 33, L17403, doi:10.1029/2006GL026972, 2006.

Zhuang, Q., Melillo, J., Mcguire, A., Kicklighter, D., Prinn, R. G., Steudler, P. A., Felzer, B. S. and Hu, S.: Net emissions of CH_4 and CO_2 in Alaska: Implications for the region's greenhouse gas budget, Ecolog. Appl., 17, 203-212, 2007.

Zhuang, Q., Chen, M., Xu, K., Tang, J., Saikawa, E., Lu, Y., Melillo, J. M., Prinn, R.

G., and McGuire, A. D.: Response of global soil consumption of atmospheric methane to changes in atmospheric climate and Nitrogen deposition. Global Biogeochem. Cy., 27, 650-663, 2013.

Zhu, X. D., Zhuang, Q. L., Xiang, G., Sokolov, A. and Schlosser, C. A.: Pan-Arctic land-atmospheric fluxes of methane and carbon dioxide in response to climate change over the 21st century, Environ. Res. Lett., 8, 045003, doi:10.1088/1748-9326/8/4/045003, 2013.

Table 1 Regional CH_4 emissions and the wetland area

		Region CH_4 emissions[$] (Tg)						Area[*] (M ha)					
		I	II	III	IV	V	China	I	II	III	IV	V	China
Inland Wetland	1950	2.80	0.31	0.25	0.06	0.11	3.53	12.26	4.78	2.66	0.30	0.27	20.27
	1980	2.06	0.27	0.22	0.06	0.10	2.71	9.71	4.61	2.57	0.29	0.26	17.44
	1990	1.90	0.23	0.14	0.09	0.08	2.44	7.73	3.42	1.77	0.44	0.18	13.54
	2000	1.13	0.23	0.13	0.05	0.07	1.61	5.40	3.43	1.41	0.23	0.15	10.62
	2010	1.16	0.22	0.12	0.05	0.06	1.61	5.09	3.20	1.36	0.20	0.13	9.98
	Decrease[#]	-58.6%	-29.0%	-50.40%	-16.7%	-45.5%	-54.4%	-58.2%	-33.3%	-48.1%	-33.3%	-66.7%	-50.8%
Coastal Wetland	1950	--	--	--	0.09	0.18	0.27	--	--	--	1.52	1.02	2.54
	1980	--	--	--	0.08	0.09	0.17	--	--	--	0.78	0.53	1.31
	1990	--	--	--	0.05	0.07	0.12	--	--	--	0.75	0.4	1.15
	2000	--	--	--	0.05	0.06	0.11	--	--	--	0.54	0.37	0.91
	2010	--	--	--	0.06	0.04	0.10	--	--	--	0.53	0.27	0.80
	Decrease[#]	--	--	--	-33.3%	-77.8%	-62.9%	--	--	--	-65.1%	-73.5%	-68.5%
Lakes and Rivers	1950	0.08	0.29	0.08	0.22	0.04	0.70	1.38	5.19	1.49	4.05	0.68	12.79
	1980	0.07	0.26	0.07	0.20	0.03	0.62	1.20	4.62	1.27	3.55	0.56	11.21
	1990	0.05	0.22	0.04	0.13	0.03	0.47	0.91	3.83	0.78	2.32	0.51	8.35
	2000	0.04	0.22	0.04	0.11	0.03	0.45	0.76	3.87	0.77	1.93	0.61	7.94
	2010	0.04	0.25	0.04	0.07	0.04	0.44	0.79	4.32	0.78	1.31	0.65	7.85
	Decrease[#]	-50.0%	-13.8%	-50.0%	-68.2%	0.0%	-37.1%	-42.8%	-16.8%	-47.7%	-67.7%	-4.4%	-38.6%
Total Wetland	1950	2.88	0.60	0.33	0.37	0.33	4.50	13.64	9.97	4.15	5.87	1.97	35.60
	1980	2.13	0.53	0.29	0.34	0.22	3.50	10.91	9.23	3.84	4.62	1.35	29.96
	1990	1.95	0.45	0.18	0.27	0.18	3.03	8.64	7.25	2.55	3.51	1.09	23.04
	2000	1.17	0.45	0.17	0.21	0.16	2.17	6.16	7.3	2.18	2.7	1.13	19.47
	2010	1.20	0.47	0.16	0.18	0.14	2.15	5.88	7.52	2.14	2.04	1.05	18.63
	Decrease[#]	-58.3%	-23.3%	-51.5%	-51.4%	-57.6%	-52.2%	-56.9%	-24.6%	-48.4%	-65.3%	-46.7%	-47.7%

[$] The average CH_4 fluxes of three consecutive years (including 1950—1952, 1979—1981, 1989—1991, 1999—2001 and 2008—2010) were used to calculated regional CH_4 emissions. For example, regional CH_4 emissions in 1980 were the production of the area of 1980 and the average CH_4 fluxes from 1979 to 1981.

[*] Data of 1980, 1990, 2000 and 2010 were from the remote sensing data (Niu et al., 2012). The area of 1978 and 2008 were regarded as the area of 1980 and 2010, respectively.

[#] Decrease means the reduce fraction in 2010 compared with 1950.

-- little or no wetland

Table 2 Estimation of CH_4 emissions from natural wetland in China.

Region	This study			Other studies			References
	CH_4 (Tg)	Period	Area (Mha)	CH_4 (Tg)	period	Area (Mha)	
China$^{\$}$	3.0	1990	23.0	2.2	1988—2000	Nm	Wang et al., 1993
China$^{\$}$	3.0	1990	23.0	1.7	1988	Nm	Khalil et al., 1993
China$^{\$}$	3.0	1990	23.0	2.0	1996	18.7	Jin et al., 1999
China$^{\$}$	3.0	1990	23.0	10.5	1990s	38.0	Wang et al., 2012b
China$^{\$}$	3.0	1990	23.0	6.65	1990	35.5	Cai, 2012
China$^{\$}$	2.2	2000	19.5	5.71	2000	30.5	Cai, 2012
China$^{\$}$	2.2	2000	19.5	3.15	2000	Nm	Chen et al., 2013
China$^{\$}$	2.2	2000	19.5	4.76	2003—2009	9.0	Zhang et al., 2013
China$^{\#}$	3.5	1950	20.3	3.2	1950	17.9	Xu and Tian, 2012
China$^{\#}$	2.7	1980	17.4	2.3	1980	13.0	Xu and Tian, 2012
China$^{\#}$	2.4	1990	13.5	2.0	1990	11.0	Xu and Tian, 2012
China$^{\#}$	1.6	2000	10.6	1.9	2000	9.4	Xu and Tian, 2012
China$^{\#}$	1.6	2010	10.0	1.9	2008	9.4	Xu and Tian, 2012
China$^{\#}$	1.6	2000	10.6	1.9	1995—2004	9.4	Tian et al., 2011
China$^{\#}$	1.6	2000	10.6	1.8	1995—2004	9.4	Ding and Cai, 2007
NYC$^{\#}$	2.8	1950	12.3	2.2	1950	10.1	Xu and Tian, 2012
NYC$^{\#}$	1.2	2010	5.1	1.2	2008	4.7	Xu and Tian, 2012
NYC$^{\#}$	1.1	2000	5.4	1.2	2001—2002	2.8	Ding et al., 2004
NYC$^{\#}$	1.1	2000	5.4	0.9	2000	Nm	Chen et al., 2013
QHT$^{\#}$	0.3	1950	4.8	0.07	1950	0.8	Xu and Tian, 2012
QHT$^{\#}$	0.2	2008	3.2	0.06	2008	0.6	Xu and Tian, 2012
QHT$^{\$}$	0.45	1990	7.3	0.8	1996	3.5	Jin et al., 1999
QHT$^{\#}$	0.23	2000	3.4	0.56	2001—2002	4.8	Ding et al., 2004
QHT$^{\#}$	0.23	2000	3.4	1.25	2000	Nm	Chen et al., 2013

[$] Natural wetland

[#] Natural wetland exclude coastal wetland, lakes and rivers.

Nm, not mentioned in the literature

NYC, Northeast China

QTH, Qinghai Tibetan Plateau

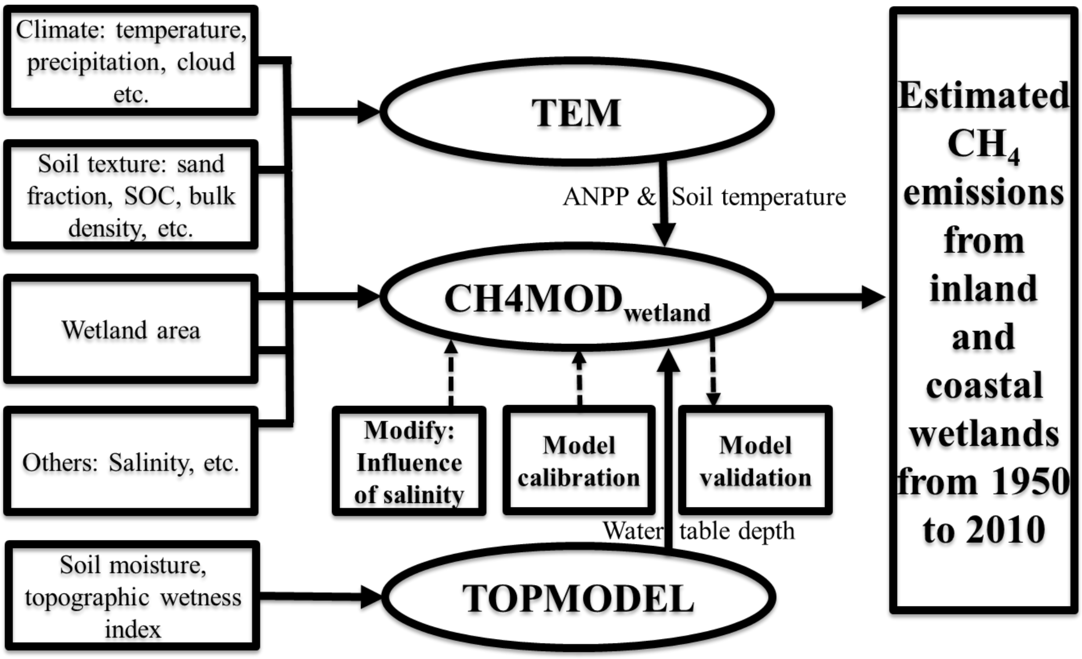

Fig. 1 Framework of simulating CH_4 emissions from inland and coastal wetlands between 1950 and 2010. $\text{CH4MOD}_{\text{wetland}}$ is a biogeophysical model to simulate CH_4 fluxes from natural wetlands. TEM is a process-based biogeochemistry model that couples carbon, nitrogen, water, and heat processes in terrestrial ecosystems to simulate ecosystem carbon and nitrogen dynamics. TOPMODEL is a conceptual rainfall-runoff model that is designed to work at the scale of large watersheds using the statistics of topography.

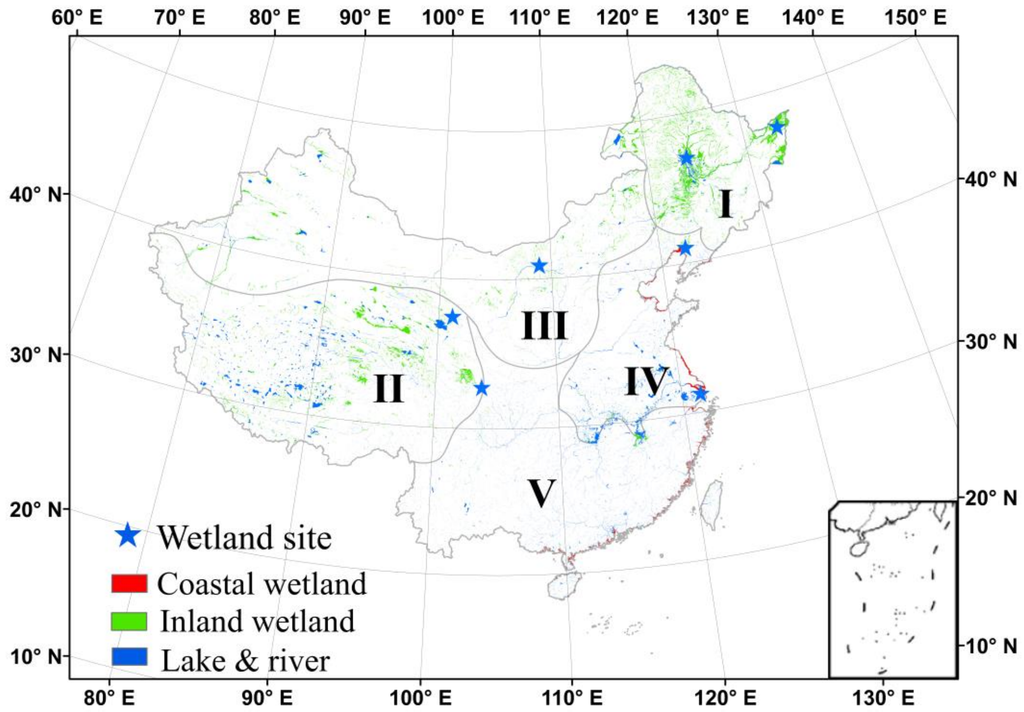

Fig. 2 Wetland regions across China. The blue stars are the locations of the wetland sites. The wetland distribution map is from the remote sensing data in 1978.

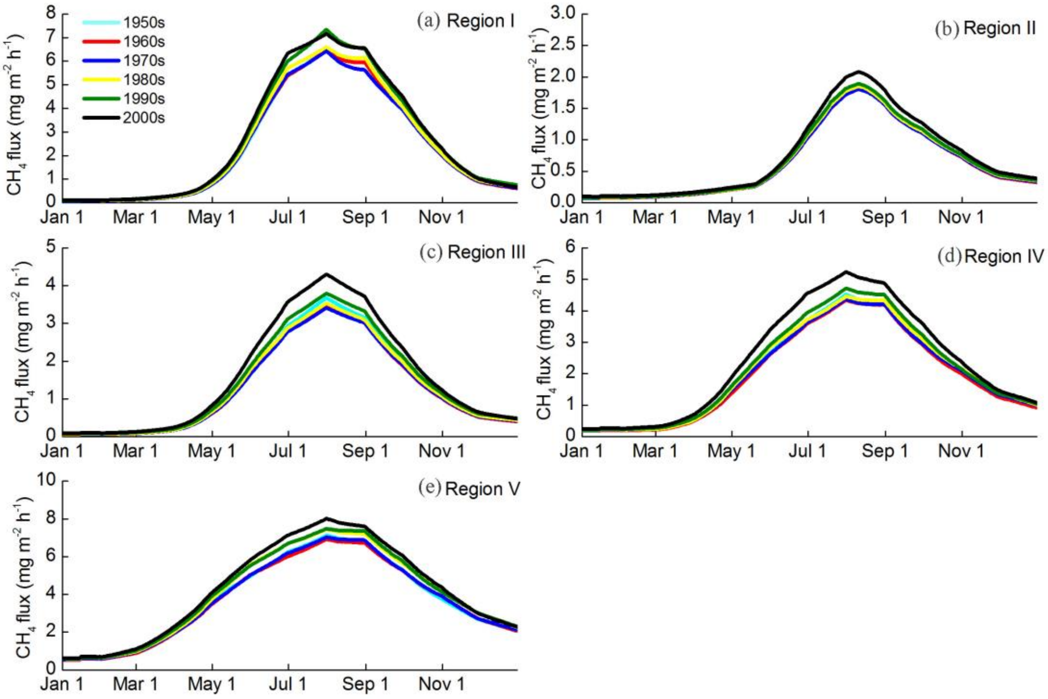

Fig. 3 Seasonal variations of methane fluxes in the five regions.

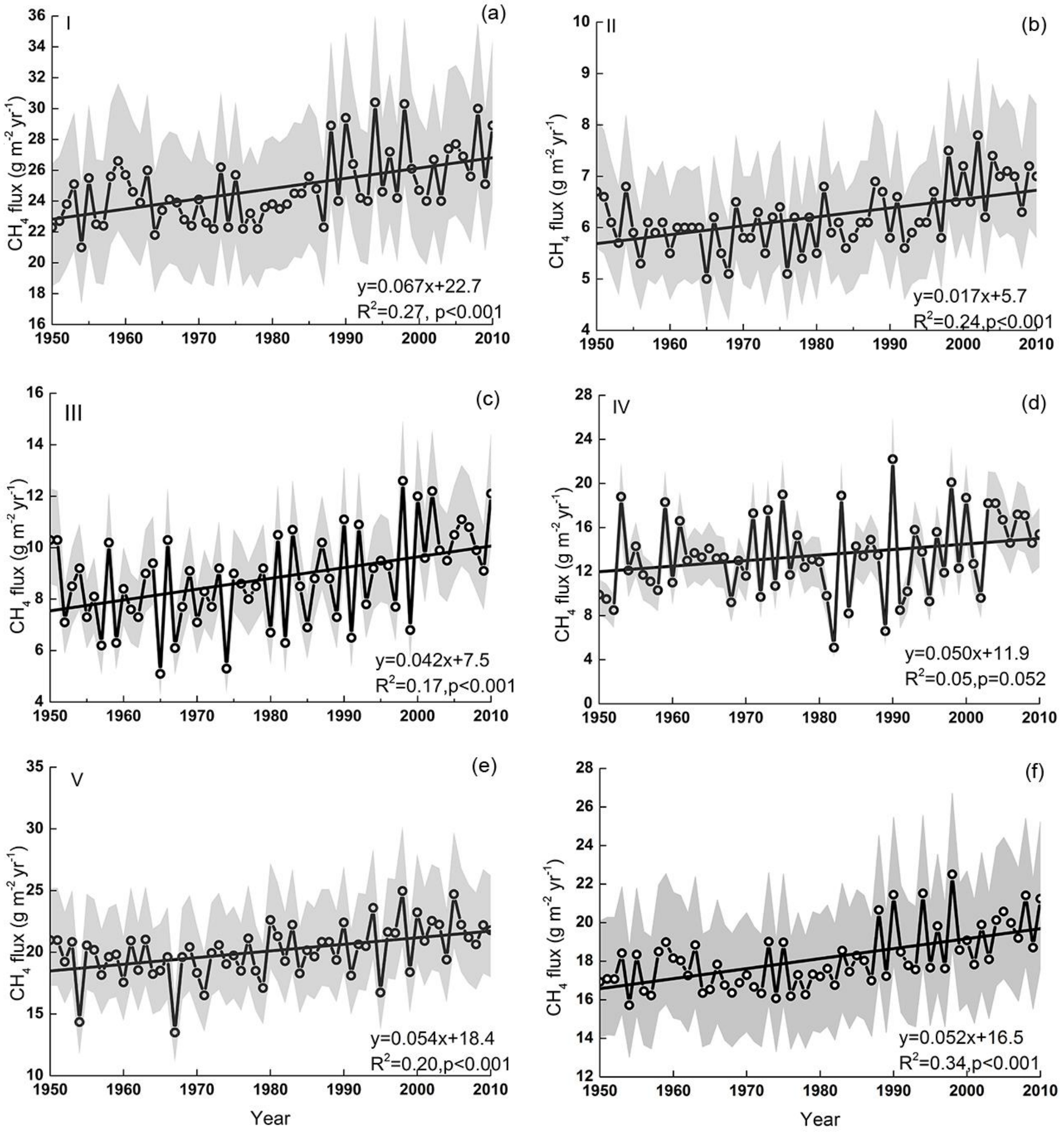

Fig. 4 Methane fluxes from inland and coastal wetlands between 1950 and 2010 in: (a) Region I; (b) Region II; (c) Region III; (d) Region IV; (e) Region V. (f) China.

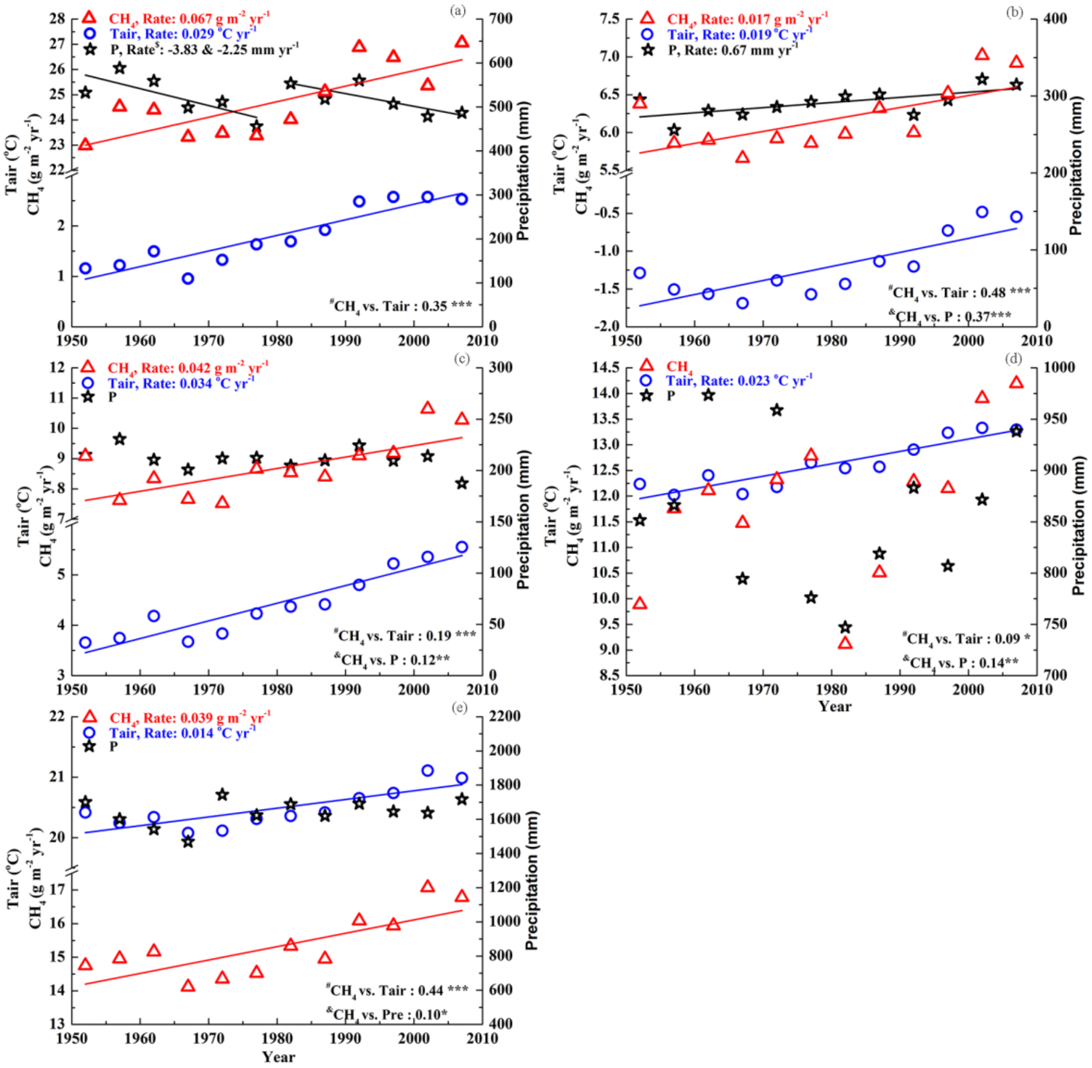

Fig. 5 Impact of the climate factors on CH_4 fluxes from 1950 to 2010 in: (a) Region I; (b) Region II; (c) Region III; (d) Region IV; and (e) Region V. The red triangles, blue circles and the black stars are 5-year average CH_4 fluxes (the same data as in Fig. 4), air temperature and precipitation, respectively. The slope represents the significant linear rate ($p<0.05$). CH_4 vs. Tair: the correlation coefficient between the annual mean CH_4 fluxes and air temperature. CH_4 vs. P: the correlation coefficient between the annual mean CH_4 fluxes and the precipitation. Only correlations with statistical significance are shown ($p<0.05$).